RM No. L6H21

NACA

RESEARCH MEMORANDUM

for the

Bureau of Aeronautics, Navy Department

EFFECT OF AN AUXILIARY BELLY FUEL TANK ON THE LOW-SPEED STATIC STABILITY CHARACTERISTICS OF A 1/5-SCALE MODEL OF THE GRUMMAN XF8F-1 AIRPLANE

TED NO. NACA 2384

By

Charles B. Cook

Langley Memorial Aeronautical Laboratory
Langley Field, Va.

NATIONAL ADVISORY COMMITTEE FOR AERONAUTICS

WASHINGTON

OCT 15 1946

NATIONAL ADVISORY COMMITTEE FOR AERONAUTICS

RESEARCH MEMORANDUM

for the

Bureau of Aeronautics, Navy Department

EFFECT OF AN AUXILIARY BELLY FUEL TANK ON THE LOW-SPEED STATIC STABILITY CHARACTERISTICS OF A 1/5-SCALE MODEL OF THE GRUMMAN XF8F-1 AIRPLANE

TED NO. NACA 2384

By Charles B. Cook

SUMMARY

In order to determine the aerodymanic effects of an auxiliary belly fuel tank on the Grumman F8F-1 airplane, a wind-tunnel investigation was made on a 1/5-scale model of the Grumman XF8F-1 airplane. Pitch and yaw tests were made with the model in the cruising and landing configurations for windmilling and take-off power conditions. Tuft studies and static-pressure measurements were also made to determine the flow characteristics in the region of the fuel tank.

It was found that, at low speed, the auxiliary fuel tank slightly improved the static longitudinal stability in most of the test conditions, especially with power on in the landing configuration at high lift coefficients. The static directional stability was decreased for most test conditions, but the addition of a fairing between the fuselage and fuel tank improved the directional stability slightly in the power-on clean condition. The effective dihedral and lateral force were increased for most of the conditions tested. The tuft studies and pressure measurements indicated that the removal of the sway braces would improve the flow characteristics considerably in the region of the fuel tank and might also decrease the buffeting of the belly tank at high speeds.

INTRODUCTION

At the request of the Bureau of Aeronautics, wind-tunnel tests were made to determine the effect of an external belly tank on the static stability characteristics of a 1/5-scale model of the Grumman XF8F-1 airplane.

The need for increasing the range of the present-day airplane has necessitated carrying a portion of the fuel in auxiliary tanks installed on the exterior of the airplane. Such installations, in some cases, have had detrimental effects on the flying qualities of the airplane.

This paper presents the results of low-speed static longitudinal and lateral stability tests, fuel-tank pressure-distribution measurements and tuft studies to obtain the effect of a universal external belly tank and belly-tank fairing on the stability characteristics of a 1/5-scale model of the Grumman XF8F-1 airplane.

COEFFICIENTS AND SYMBOLS

The results of the tests are presented as standard NACA coefficients of forces and moments. Rolling-, yawing-, and pitching-moment coefficients are given about the center-of-gravity location shown in figure 1 (24.64 percent of the mean aerodynamic chord). The data are referred to the stability axes, which are a system of axes having their origin at the center of gravity and in which the Z-axis is in the plane of symmetry and perpendicular to the relative wind, the X-axis is in the plane of symmetry and perpendicular to the Z-axis, and the Y-axis is perpendicular to the plane of symmetry. The positive directions of the stability axes, of angular displacements of the airplane and control surfaces are shown in figure 2.

The coefficients and symbols are defined as follows:

C_L lift coefficient (Lift/qS)

C_X longitudinal-force coefficient (X/qS)

C_Y lateral-force coefficient (Y/qS)

C_l rolling-moment coefficient (L/qSb)

C_m pitching-moment coefficient (M/qSc')

C_n yawing-moment coefficient (N/qSb)

T_c' effective thrust coefficient based on wing area $\left(T_{eff}/qS\right)$

Lift = -Z

X, Y, Z } forces along axes, pounds

L, M, N } moments about axes, pound-feet

T_{eff} propeller effective thrust, pounds

q free-stream dynamic pressure, pounds per square foot $\left(\frac{\rho V^2}{2}\right)$

q_s slipstream dynamic pressure, pounds per square foot

p static pressure at survey station

p_o free-stream static pressure

S wing area (9.76 sq ft on model)

S_t horizontal tail area (2.06 sq ft on model)

c' wing mean aerodynamic chord (M.A.C.) (1.460 ft on model)

b wing span (7.10 ft on model)

V air velocity, feet per second

D propeller diameter (2.52 ft on model)

and

ρ mass density of air, slugs per cubic foot

α angle of attack of thrust line, degrees

ψ angle of yaw, degrees

i_t angle of stabilizer with respect to thrust line, degrees; positive when trailing edge is down

i_f angle of fin with respect to thrust line, degrees; positive when nose of fin moves to right (-2° on model)

δ control-surface deflection, degrees

β propeller blade angle at 0.75 radius (20° on model)

n_o tail-off aerodynamic-center location, percent wing mean aerodynamic chord

n_p neutral-point location, percent wing mean aerodynamic chord (center-of-gravity location for neutral stability in trimmed flight)

Subscripts:

e elevator

r rudder

f flap

ψ denotes partial derivatives of a coefficient with respect to yaw $\left(\text{example: } C_{l_\psi} = \frac{\partial C_l}{\partial \psi}\right)$

MODEL AND APPARATUS

The model was an old model of the Grumman XF8F-1 airplane on which previous tests had been run. A three-view drawing of the model with the belly tank installed is given in figure 1, and figure 3 shows the model installed in the tunnel. A more complete description of the model can be found in references 1 and 2.

The belly tank was a 1/5-scale model of the "Universal" 150 gallon tank that is used on numerous other airplanes, and was a symmetrical streamline body with a length of 26.40 inches and a maximum diameter of 4.73 inches. The fairing between the belly tank and fuselage was a symmetrical airfoil section with a maximum thickness of 16.4 percent of the chord at the 38.4 percent chord

point based on an average chord of 14.6 inches. The sway braces were made from 1/4-inch-diameter tubing. Details of the belly tank and sway braces are shown on figure 4. Figure 5 shows the belly-tank fairing installation.

The flow in the region of the belly tank was observed by means of tufts placed around the entire belly tank and on the underside of the fuselage. For the belly tank with fairing tests, tufts were also placed over the entire fairing.

The pressure survey on the belly tank and on the underside of the fuselage in the vicinity of the belly tank was obtained by the use of 0.035-inch-diameter static-pressure tubes placed approximately one tube diameter away from and parallel to the surface. Only one station (distance from nose of tank) was surveyed at a time after which all the tubes were moved back to the next station. The location of the static-pressure tubes is shown in figure 6.

All tests were made with propeller installed, the power being obtained from a 56-horsepower electric motor, the speed of which was determined from an electric tachometer the accuracy of which is within ±0.2 percent.

The model was tested in the Langley 7- by 10-foot tunnel. The model configurations referred to in the text and in the figures were as follows:

(a) Cruising configuration

Flaps retracted
Landing gear retracted
Landing-gear door closed

(b) Landing configuration

Flaps deflected 40°
Landing gear extended
Landing-gear door open

No restriction was placed upon the flow of air from the wing inlet ducts through the exit openings for all the stability tests. For the pressure-survey tests the flow of air from the wing inlet ducts was sealed off at the oil-cooler exit openings to make the test results more general. Because of time limitations no pressure survey tests were run with the flow of air from the wing inlet ducts unsealed at the oil cooler.

TESTS AND RESULTS

Test Conditions

The tests were made at dynamic pressures of 6.39, 9.21, and 16.37 pounds per square foot, which correspond to airspeeds of about 50, 60, and 80 miles per hour. The test Reynolds numbers were about 680,000, 820,000, and 1,090,000 based on the wing mean aerodynamic chord of 1.46 feet. Because of the turbulence factor of 1.6 for the tunnel, the effective Reynolds numbers (for maximum lift coefficients) were about 1,090,000, 1,310,000, and 1,750,000.

Corrections

Because of the presence of the belly tank, the model was tested in an inverted position. None of the data have been corrected for tares caused by the model support strut. Jet-boundary corrections have only been applied to the angles of attack and the drag coefficients. The following correction were added to the test data:

$$\Delta\alpha = 57.3\ \delta_w \frac{S}{C} C_L \text{ (degrees)}$$

$$\Delta C_X = -\delta_w \frac{S}{C} C_L^2$$

where

δ_w jet-boundary correction factor at the wing (0.115)

C tunnel cross-sectional area (69.59 sq ft)

Test Procedure

The model was equipped with a propeller having three blades instead of four as on the full-scale airplane. A complete description of the propeller plan form, propeller calibration, and the variation of effective thrust coefficient with lift coefficient can be found in reference 1.

The longitudinal-stability data presented herein were obtained throughout the pitch range with tail off and with two stabilizer settings for each of the two model configurations.

Lateral-stability derivatives were obtained from pitch tests at angles of yaw of $\pm 5^\circ$ by assuming a straight-line variation between these points. The large-symbol points on the plots of lateral-stability derivatives were obtained by measuring slopes through zero yaw from yaw tests.

At each angle of attack for power-on yaw tests the propeller speed was held constant throughout the yaw range. Since the lift and thrust coefficients vary with yaw when the propeller speed and angle of attack are held constant, the thrust coefficient is strictly correct only at zero yaw.

All the tuft tests were made in the cruising configuration at an angle of attack corresponding to an airplane lift coefficient of 0.250.

The pressure tests on the belly tank were made in the cruising configuration for a take-off power condition. The pressure tests were made with the belly-tank sway braces off at lift coefficients of 0.250, 0.365, 0.450, and angles of yaw of 0° and $\pm 5^\circ$. The pressure tests with the sway braces on were made at a lift coefficient of 0.250 and at zero yaw. Upon completion of the pressure tests the data obtained from tube No. 5 appeared to be erratic and unreliable and consequently are not presented in the report.

All the tests were made with the model inverted and since no tares were applied the data are valid only insofar as increments are concerned. The signs of all coefficients and angles are presented so that the data may be applied to the airplane in the usual sense. (See fig. 2.)

All the stability tests were run in pairs, one with the belly tank installed and one with the belly tank removed. The ailerons, rudder, and elevators were set at 0° for all tests.

Presentation of Results

An outline of the figures presenting the results is given as follows:

DISCUSSION

Longitudinal Stability

The effect of the belly tank on the static longitudinal stability of the model, with windmilling propeller or take-off power is to increase the longitudinal stability a slight amount for the cruising configuration (fig. 8). For the landing configuration the effect of the belly tank is to decrease slightly the longitudinal stability at low lift coefficients and to increase slightly the longitudinal stability at high lift coefficients.

The increment in aerodynamic-center location owing to the belly tank (fig. 8) indicates that the tank causes little change in the air flow at the horizontal tail surfaces.

It should be noted that the pitching-moment coefficients have been referred to the tank-off center-of-gravity location in order to obtain the aerodynamic effect of the tank. The tests indicated that the fuel tank would not change the neutral-point location more than 3 percent of the mean aerodynamic chord in either a forward or rearward direction. The presence of a full belly tank will shift the neutral-point location with take-off power rearward approximately 3 percent of the mean aerodynamic chord. This is based on calculations taking into account the thrust of the propeller and the vertical shift of the center-of-gravity location caused by the full belly tank.

Lateral Stability

The effect of an external belly tank and belly-tank fairing on the lateral-stability parameters is given in figures 9 and 10 and summarized in table I. The tank-off stability parameters C_{Y_ψ}, C_{n_ψ}, and C_{l_ψ} presented in table I were taken from reference 2 where the jet-boundary and tare corrections were applied to the data and the tail surfaces installed on the model. The increments in the lateral stability parameters resulting from the belly tank and belly-tank fairing presented in this table were obtained from present test data with the tail surfaces removed. The effect of removing the tail surfaces, at small angles of yaw, on the incremental values of C_Y, C_n, and C_l caused by the belly tank are negligible (fig. 11). Thus the total lateral-stability parameters obtained by adding the tail-on parameters (from reference 2) to the tail-off increments resulting from the belly tank and belly-tank fairing are justified.

Directional stability.- The data with windmilling propeller show that the belly tank produced a positive increment in C_{n_ψ} at high lift coefficients reducing to zero at low lift coefficients for the cruising configuration (fig. 9(a)) and higher positive increments in C_{n_ψ} for the landing configuration (fig. 10(a)). The addition of the belly-tank fairing had no effect on C_{n_ψ} with the model in the cruising configuration (the only configuration which the belly-tank fairing was tested) with windmilling propeller (fig. 9(a)).

The data with take-off power indicate that the belly tank had no appreciable effect on C_{n_ψ} with the model in the landing configuration (fig. 10(b)); however, in the cruising configuration the belly tank caused a slight positive increment in C_{n_ψ} at low lift coefficients and increasing more positively at higher lift coefficients (fig. 10(b)). The addition of the belly-tank fairing improved the directional stability of the model for the cruising configuration and take-off power condition (fig. 10(b)).

Effective dihedral.- The effective dihedral ($C_{l_\psi} = 0.0002$ is approximately equivalent to 1° effective dihedral) was increased about 3/4° by the addition of the belly tank for both the cruising and landing configurations in the windmilling condition (figs. 9(a) and 10(a)). The addition of the fairing increased the effective dihedral even more at high lift coefficients in the cruising configuration (the only configuration in which the fairing was tested) and windmilling condition (fig. 9(a)). The probable reason for the

increase in effective dihedral is that the belly tank and fairing increases the depth of the fuselage or effectively raises the wing position. It is well known that raising the wing will result in increased effective dihedral (reference 3).

The belly tank had no appreciable effect on C_{l_ψ} with the model in the landing configuration with take-off power (fig. 10(b)). In the cruising configuration with take-off power the belly tank decreased the effective dihedral. No logical reason can be given for this decrease in effective dihedral except that it might be due to some adverse flow condition resulting from the slipstream. The addition of the belly-tank fairing in the cruising configuration with take-off power increased the effective dihedral.

Lateral force.- The belly tank produced a positive increase in the lateral-force parameter for all the conditions tested (figs. 9, 10, and 11). The reason for this increase in the lateral-force parameter is selfevident in that with an increase in side area would be expected to increase the lateral force. The addition of the fairing did not affect the lateral-force parameter.

Air-Flow Studies

Tuft tests with tank fairing and sway braces on and propeller windmilling indicated turbulent flow in the region from the midpoint of the belly-tank fairing to the end of the fairing while the region from the midpoint of the fairing to the nose of the fairing slightly turbulent flow was indicated. The flow was unsteady on the belly tank in the region between the center line of the tank and edge of the belly-tank fairing. The take-off power condition showed a slight improvement in the air flow.

The windmilling condition with the belly-tank fairing removed disclosed that the region of the belly tank and fuselage aft of the rear sway braces was in a turbulent flow condition. This turbulent flow condition accompanied by buffeting of the fuel tank was also obtained in some unpublished NACA flight tuft tests of an F8F airplane with a similar installation. The air flow on the sides of the belly tank including the area between the belly-tank center line and the rear sway brace to the end of the tank was in a slightly turbulent flow condition. Applying take-off power had a slight improving effect on the air-flow characteristics.

For the windmilling condition with the fairing on and sway braces removed the tufts in the region from the midpoint of the fairing to the end of the fairing indicated a slightly turbulent

flow condition. Application of take-off power did not change the flow characteristics.

The tuft tests with the belly-tank fairing removed and the sway braces removed indicated a smooth flow condition on the belly tank and in the region between the belly tank and the underside of the fuselage.

It should be noted that the tests were made at low values of Reynolds number and Mach number. Some of the adverse flow caused by the sway braces could probably be avoided by using streamline rather than round sections in the sway braces. This in turn might also reduce some of the buffeting of the belly tank.

Pressure Distribution

The results of the pressure-distribution survey are presented in figure 12 as pressure coefficient plotted against the orifice location for various lift coefficients and angles of yaw with the belly-tank sway braces installed and removed.

From the known local low-speed pressure coefficients given in figure 12 the flight Mach number at which local sonic speed will be reached on the belly tank can be estimated by means of the von Kármán-Tsien method presented in reference 4. Strictly speaking these curves should not be used for estimating the critical Mach number because the pressure coefficient is based on a free-stream dynamic pressure rather than a slipstream dynamic pressure in which the tank was located. By using free-stream dynamic pressure instead of slipstream dynamic pressure an increase of about 5 percent is obtained in calculating the pressure coefficient, which in turn gives a corresponding decrease in the critical Mach number in the order of 5 percent. For convenience in converting the free-stream pressure coefficient to slipstream pressure coefficient the ratio of slipstream dynamic pressure to free-stream dynamic pressure is given on figure 12. The ratio of slipstream dynamic pressure to free-stream dynamic pressure was based on readings from a total-head tube placed at the nose of the tank. It is felt with the number of stations at which the static pressure was measured and the fairing of the curves that the use of the curves presented in figure 12 is justified in predicting approximate critical speeds.

The greatest effect of removing the sway braces, shown in figure 12(c), was to decrease the pressure coefficient from -1.13 to -0.09, corresponding to an increase in the critical Mach number from 0.57 to 0.89. The critical Mach number of 0.57 obtained from the low-speed pressure measurements agrees surprisingly well with the

Mach number of 0.59 obtained from NACA flight tests in which turbulent flow and violent buffeting were encountered. It should be pointed out that this correlation might be fortuitous since critical-speed estimations made from low-speed data by use of reference 4 for bodies having high sharp pressure peaks, as was the case when the sway braces were installed, may be greatly in error. The steep adverse pressure gradient which occurs after the high peak may cause boundary-layer separation before the critical Mach number is reached, which is indicated in this case by the tuft studies.

The critical Mach number estimation from the data with sway braces removed should be less fortuitous since the pressure survey indicated low broad pressure peaks and smooth flow is indicated from the tuft tests.

CONCLUSIONS

The results of low-speed wind-tunnel tests to determine the effect of an auxiliary belly fuel tank on the stability characteristics of a 1/5-scale model of the Grumman XF8F-1 airplane indicate the following conclusions:

1. For a fixed center-of-gravity location the belly tank slightly increased the longitudinal stability of the model with windmilling and take-off power for the cruising configuration. The longitudinal stability was decreased slightly at low lift coefficients and increased at high lift coefficients with the belly tank installed and the model in the landing configuration for both windmilling and take-off power conditions.

2. The directional stability was decreased by installing the belly tank for both cruising and landing configurations with the propeller windmilling. The belly tank had no appreciable effect on the directional stability in the landing configuration and take-off power condition, but in the cruising configuration the directional stability was decreased at high lift coefficients.

3. The addition of the belly-tank fairing improved the directional stability for the power-on clean conditions.

4. The effective dihedral of the model was increased by the belly tank and belly-tank fairing in all conditions tested except the take-off power condition with the model in the cruising configuration.

5. The lateral force was increased with the belly tank on the model for all test conditions.

6. The tuft studies indicated that the presence of the sway braces caused turbulent flow conditions, the addition of a relatively thick fairing between the fuselage and belly tank caused little improvement in the flow, and the application of take-off power caused a slight improvement in the flow.

7. The sway braces caused high sharp peaks in the pressure distribution around the tank.

Langley Memorial Aeronautical Laboratory
National Advisory Committee for Aeronautics
Langley Field, Va.

Charles B. Cook
Charles B. Cook
Aeronautical Engineer

Approved: Joseph A. Shortal
for Hartley A. Soulé
Chief of Stability Research Division

CMH

REFERENCES

1. Riebe, John M., and Spear, Margaret F.: Wind-Tunnel Tests of a 1/5-Scale Powered Model of the Grumman XF8F-1 Airplane. II - Longitudinal Stability and Control - TED No. NACA 2344. NACA MR No. L5E16, Bur. Aero., 1945.

2. Watson, James M., and Comisarow, Paul: Wind-Tunnel Tests of a 1/5-Scale Powered Model of the Grumman XF8F-1 Airplane. III - Lateral Stability and Control - TED No. NACA 2344. NACA MR No. L5F05, Bur. Aero., 1945.

3. House, Rufus O., and Wallace, Arthur R.: Wind-Tunnel Investigation of Effect of Interference on Lateral-Stability Characteristics of Four NACA 23012 Wings, an Elliptical and a Circular Fuselage, and Vertical Fins. NACA Rep. No. 705, 1941.

4. von Kármán, Th.: Compressibility Effects in Aerodynamics. Jour. Aero. Sci., vol. 8, no. 9, July 1941, pp. 337-356.

TABLE I

CONFIDENTIAL

EFFECT OF BELLY TANK AND BELLY-TANK FAIRING ON THE

LATERAL STABILITY PARAMETERS

			Tail-on data[a]			Tail-off data						Tail-on data + tail-off data					
			Tank off			Tank on[b]			Fairing on[c]			Tank off[a] + tank on[b]			Tank off[a] + tank on[b] + fairing on[c]		
Configuration	Power	C_L	C_{y_ψ}	C_{n_ψ}	C_{l_ψ}	ΔC_{y_ψ}	ΔC_{n_ψ}	ΔC_{l_ψ}	ΔC_{y_ψ}	ΔC_{n_ψ}	ΔC_{l_ψ}	C_{y_ψ}	C_{n_ψ}	C_{l_ψ}	C_{y_ψ}	C_{n_ψ}	C_{l_ψ}
Cruising	Windmilling	0.3	0.0079	-0.00087	0.00119	0.00190	0	0.00010	0	0	0.00010	0.00980	-0.00087	0.00129	0.00980	-0.00087	0.00139
Cruising	Windmilling	1.0	.0075	-.00085	.00144	.00100	.00015	.00013	0	0	.00028	.00850	-.00070	.00157	.00850	-.00070	.00185
Cruising	Take-off power	.3	.0087	-.00110	.00080	.00015	.00020	0	0	-.00009	.00010	.00885	-.00090	.00080	.00885	-.00099	.00090
Cruising	Take-off power	1.0	.0117	-.00149	.00100	.00022	.00045	-.00015	0	-.00030	.00020	.01192	-.00104	.00085	.01192	-.00134	.00105
Landing	Windmilling	.6	.0159	-.00122	.00130	.00200	0	.00017	----	-------	-------	.01790	-.00122	.00147	-------	-------	-------
Landing	Windmilling	1.5	.0152	-.00130	.00120	.00120	.00028	.00019	----	-------	-------	.01640	-.00102	.00139	-------	-------	-------
Landing	Take-off power	.6	.0197	-.00160	.00130	.00160	0	0	----	-------	-------	.02130	-.00160	.00130	-------	-------	-------
Landing	Take-off power	1.5	.0279	-.00248	-.00025	.00340	0	0	----	-------	-------	.03130	-.00248	-.00025	-------	-------	-------

[a]Data from reference 2.

[b]Increment due to addition of belly tank.

[c]Increment due to addition of fairing.

CONFIDENTIAL

NATIONAL ADVISORY
COMMITTEE FOR AERONAUTICS

NACA RM No. L6H21

FIGURE LEGENDS

Figure 1.- Three-view drawing of 1/5-scale model of Grumman XF8F-1.

Figure 2.- System of axes and control-surface hinge moments and deflections. Positive values of forces, moments, and angles are indicated by arrows.

Figure 3.- Langley 7- by 10-foot tunnel installation of $\frac{1}{5}$-scale model of Grumman XF8F-1 airplane with model of 150-gallon universal external fuel tank.

(a) Belly tank and sway braces.

Figure 3.- Concluded.

(b) Belly tank, sway braces, and fairing.

Figure 4.- Installation details of belly tank and sway braces.

Figure 5.- Belly-tank fairing installation.

Figure 6.- Section looking rearward at pressure tubes on external belly tank and underside of fuselage on a 1/5-scale model of a Grumman XF8F-1 airplane.

Figure 7.- Effect of external belly tank on the aerodynamic characteristics in pitch of a 1/5-scale model of a Grumman XF8F-1 airplane.

(a) Windmilling, cruising configuration.

Figure 7.- Continued.

(b) Take-off power, cruising configuration.

Figure 7.- Continued.

(c) Windmilling, landing configuration.

Figure 7.- Concluded.

(d) Take-off power, landing configuration.

Figure 8.- Increment in neutral point and aerodynamic center due to belly tank for a 1/5-scale model of the Grumman XF8F-1 airplane, elevator fixed and tail off.

FIGURE LEGENDS - Continued

Figure 9.- Effect of external belly tank and belly tank fairing on the parameters C_{l_ψ}, C_{n_ψ} and C_{y_ψ} of a 1/5-scale model of a Grumman XF8F-1 airplane, tail off.

(a) Windmilling, cruising configuration.

Figure 9.- Concluded.

(b) Take-off power, cruising configuration.

Figure 10.- Effect of external belly tank on the parameters C_{l_ψ}, C_{n_ψ}, and C_{y_ψ} of a 1/5-scale model of a Grumman XF8F-1 airplane, tail off.

(a) Windmilling, landing configuration.

Figure 10.- Concluded.

(b) Take-off power, landing configuration.

Figure 11.- Effect of external belly tank on the aerodynamic characteristics in yaw of a 1/5-scale model of a Grumman XF8F-1 airplane.

(a) Windmilling, cruising configuration, $\alpha \cong 11.2^\circ$.

Figure 11.- Continued.

(a) Concluded.

Figure 11.- Continued.

(b) Take-off power, cruising configuration, $\alpha \cong 2.2^\circ$.

Figure 11.- Continued

(b) Concluded.

Figure 11.- Continued.

(c) Take-off power, cruising configuration, $\alpha \cong 11.0^\circ$.

Figure 11.- Continued.

(c) Concluded.

FIGURE LEGENDS - Continued

Figure 11.- Continued.

(d) Windmilling, landing configuration, $\alpha \cong 11.7^{\circ}$.

Figure 11.- Continued.

(d) Concluded.

Figure 11.- Continued.

(e) Take-off power, landing configuration, $\alpha \cong 10.0^{\circ}$.

Figure 11.- Continued.

(e) Continued.

Figure 11.- Concluded.

(e) Concluded.

Figure 12.- Effect of sway braces, lift coefficient and angle of yaw on the pressure coefficient on an external belly tank mounted on a 1/5-scale model of a Grumman XF8F-1 airplane. Take-off power (2100 hp at 2800 rpm), cruising condition; tail off.

(a) Pressure tube no. 1.

Figure 12.- Continued.

(b) Pressure tube no. 2.

Figure 12.- Continued.

(c) Pressure tube no. 3.

Figure 12.- Continued.

(d) Pressure tube no. 4.

Figure 12.- Continued.

(e) Pressure tube no. 5.

Figure 12.- Continued.

(f) Pressure tube no. 6.

FIGURE LEGENDS - Concluded

Figure 12.- Continued.

(g) Pressure tube no. 7.

Figure 12.- Continued.

(h) Pressure tube no. 8.

Figure 12.- Continued.

(i) Pressure tube no. 9.

Figure 12.- Continued.

(j) Pressure tube no. 10.

Figure 12.- Continued.

(k) Pressure tube no. 11.

Figure 12.- Continued.

(l) Pressure tube no. 12.

Figure 12.- Continued.

(m) Pressure tube no. 13.

Figure 12.- Continued.

(n) Pressure tube no. 14.

Figure 12.- Concluded.

(o) Pressure tube no. 15.

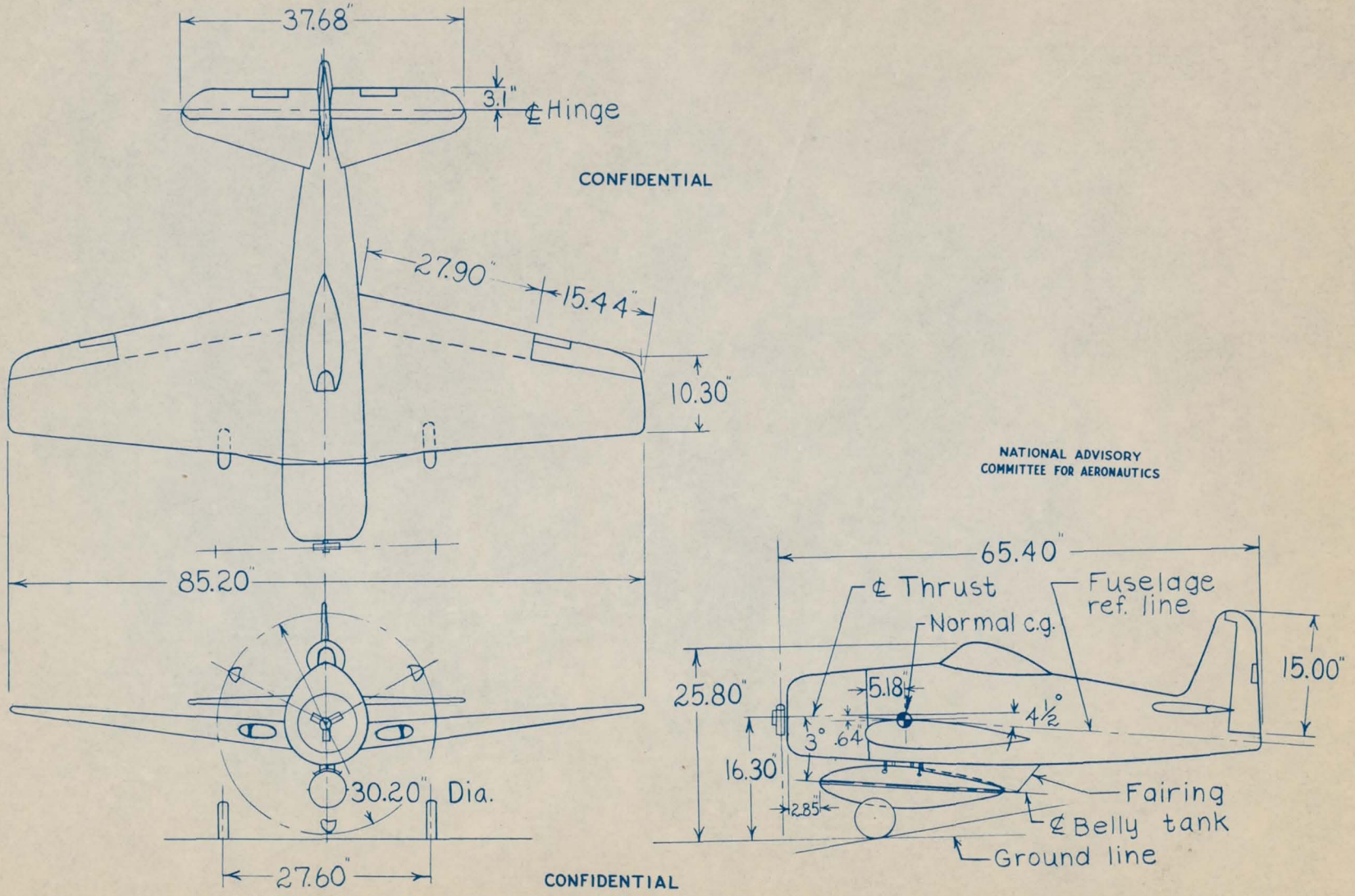

Figure 1. – Three-view drawing of 1/5 – scale model of Grumman XF8F-1

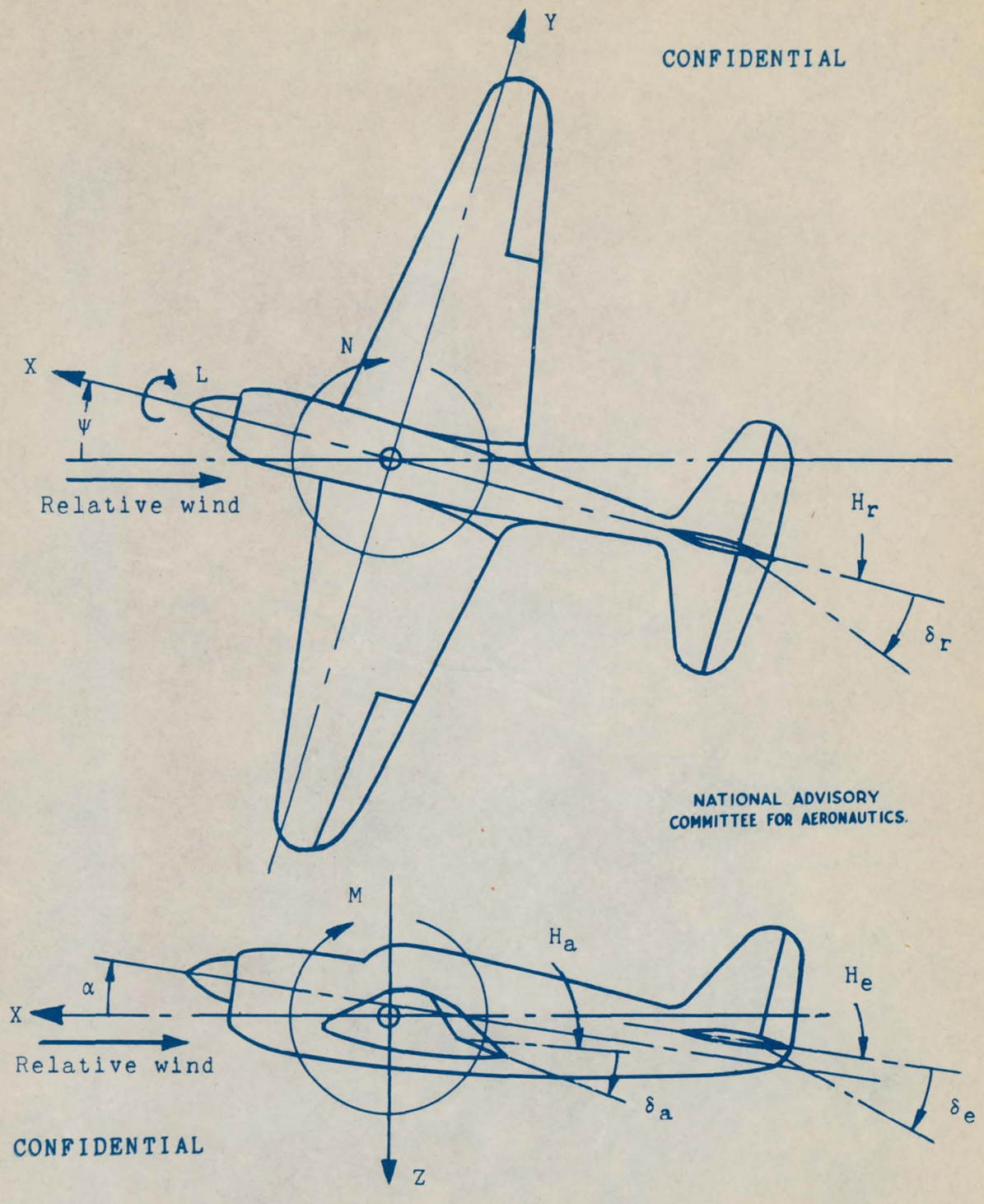

Figure 2.- System of axes and control-surface hinge moments and deflections. Positive values of forces, moments, and angles are indicated by arrows.

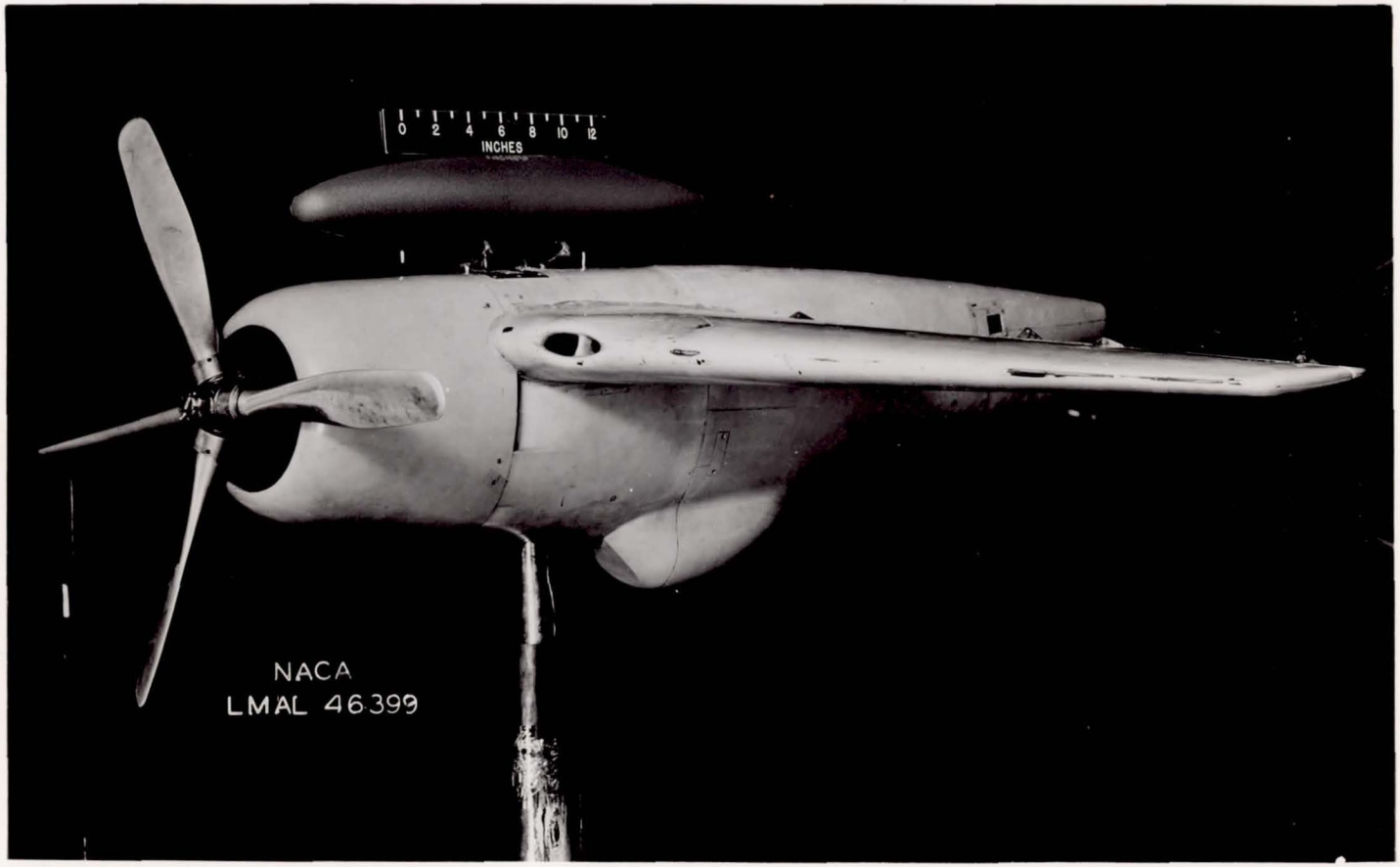

(a) Belly tank and sway braces.

Figure 3.- Langley 7- by 10-foot tunnel installation of $\frac{1}{5}$-scale model of Grumman XF8F-1 airplane with model of 150-gallon universal external fuel tank.

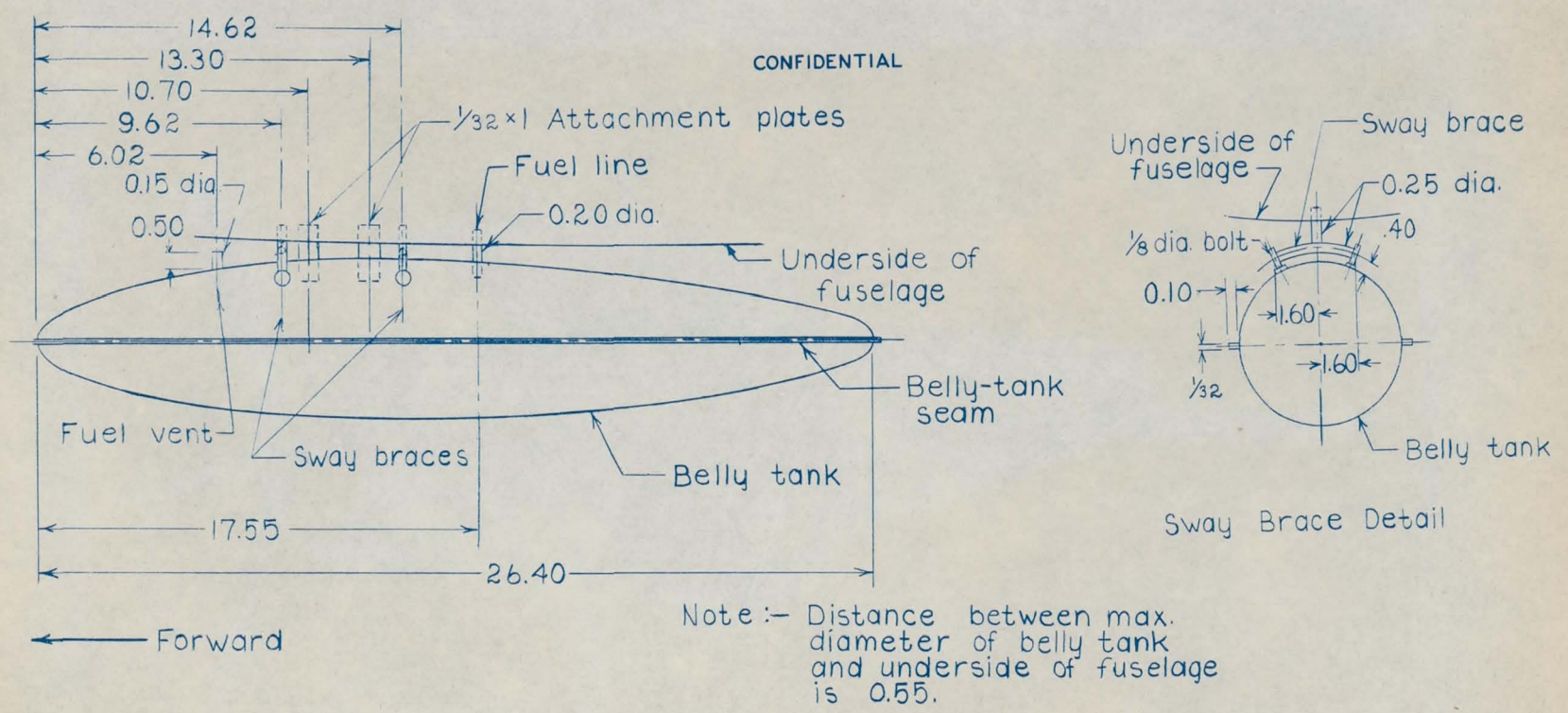

NATIONAL ADVISORY COMMITTEE FOR AERONAUTICS

Figure 4 .- Installation details of belly tank and sway braces.

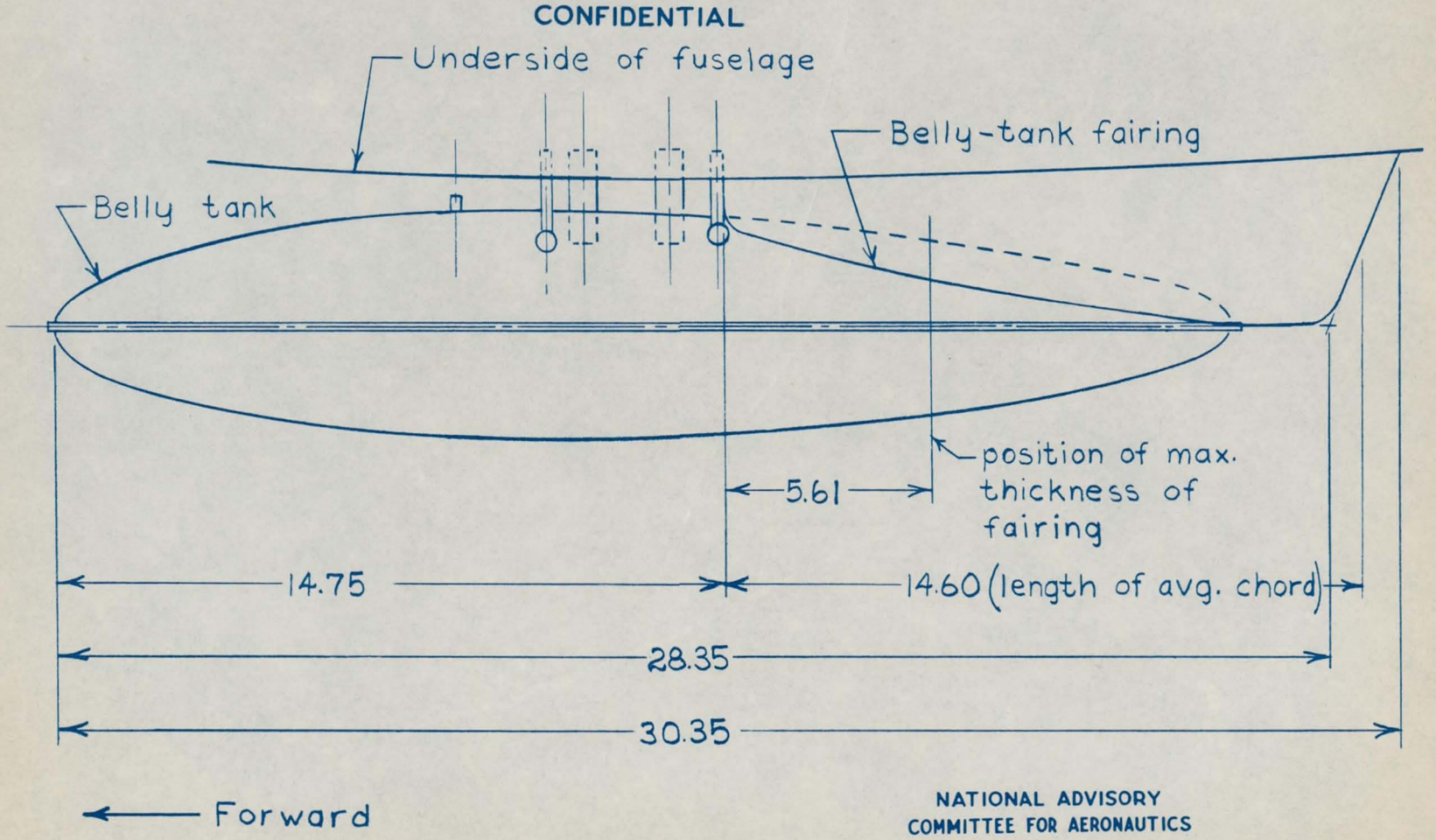

Figure 5.– Belly-tank fairing installation.

CONFIDENTIAL

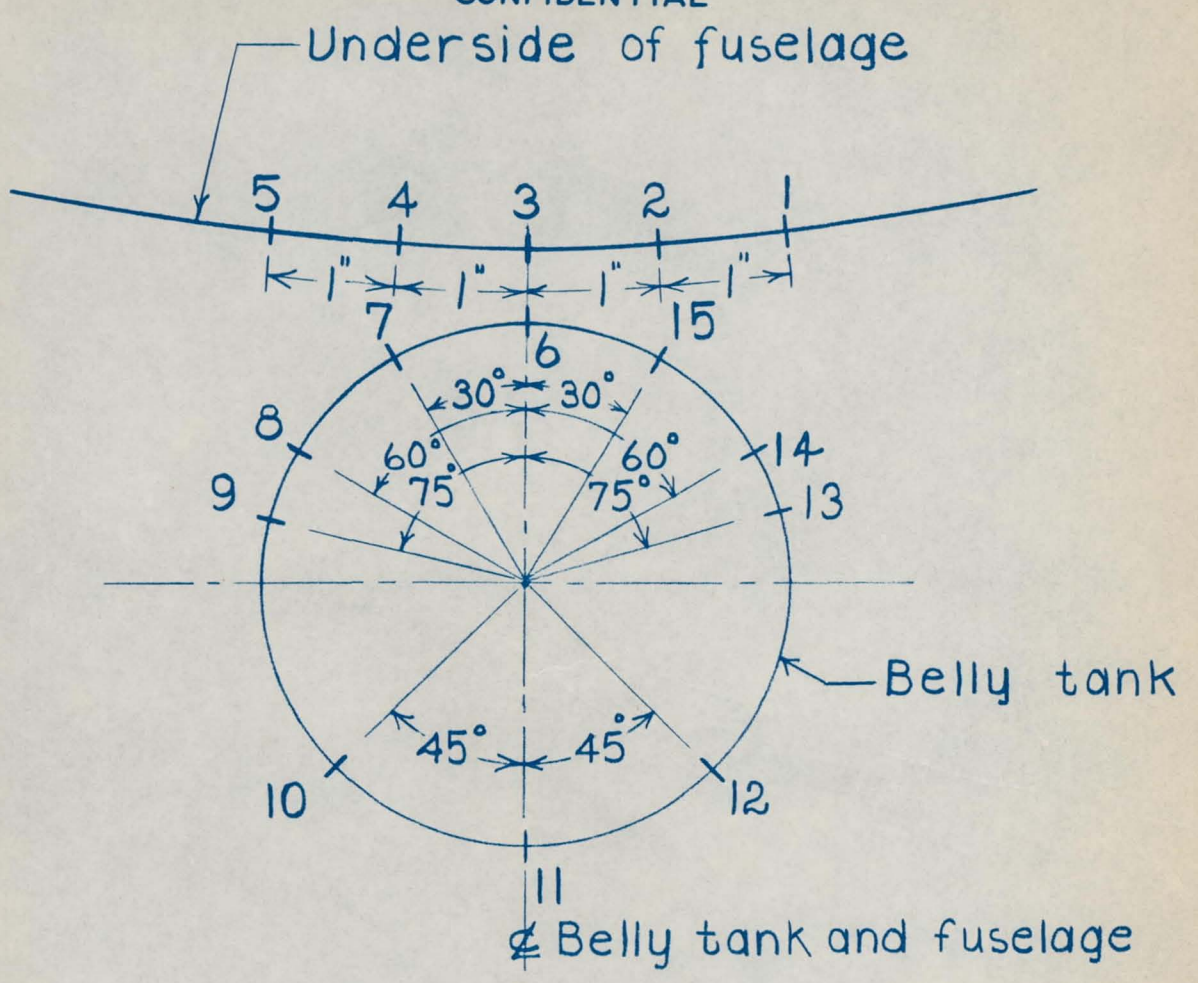

NATIONAL ADVISORY
COMMITTEE FOR AERONAUTICS

Figure 6.— Section looking rearward at pressure tubes on external belly tank and underside of fuselage on a 1/5-scale model of a Grumman XF8F-1 airplane.

CONFIDENTIAL

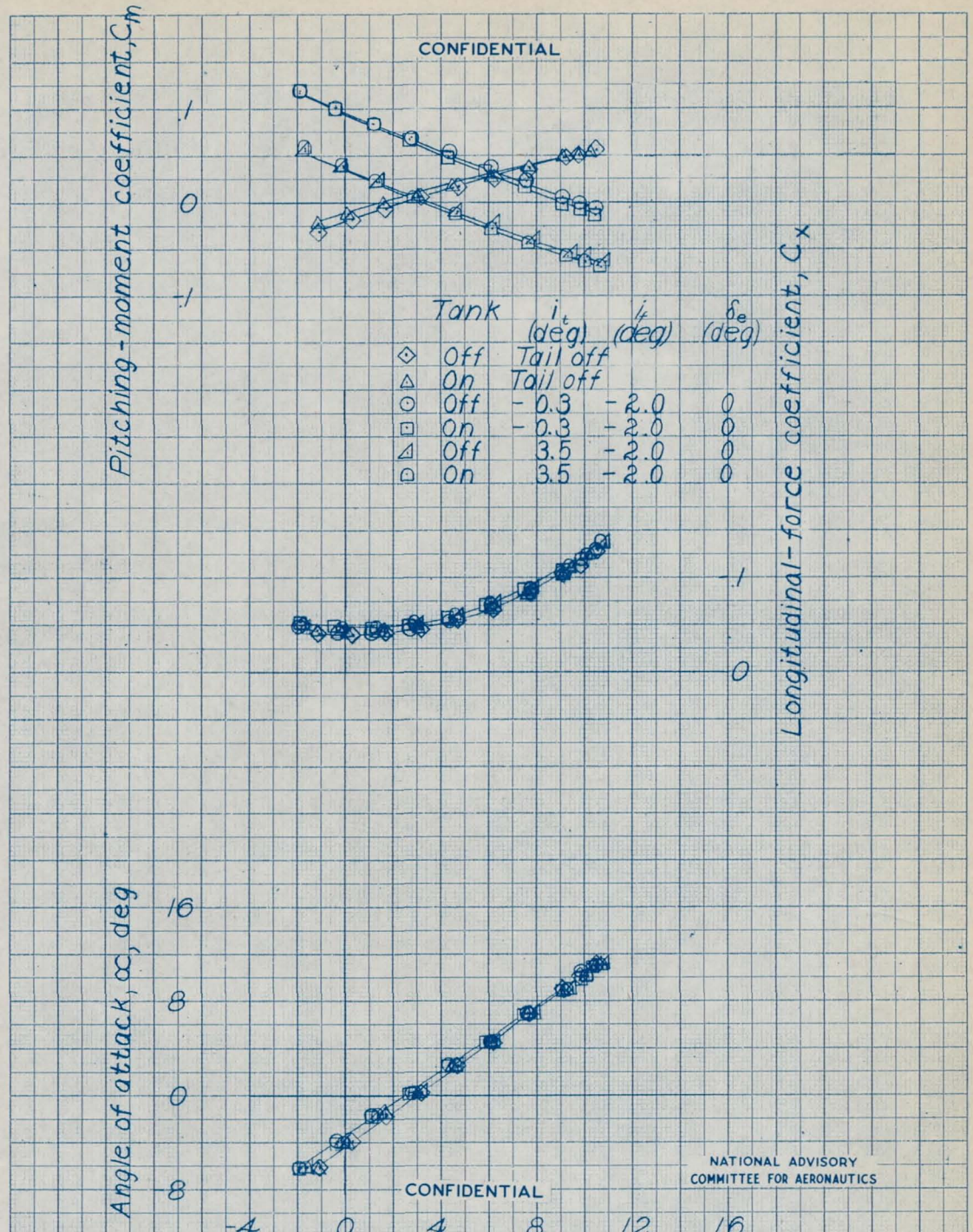

(a) Windmilling, cruising configuration.

Figure 7.- Effect of external belly tank on the aerodynamic characteristics in pitch of a 1/5-scale model of a Grumman XF8F-1 airplane.

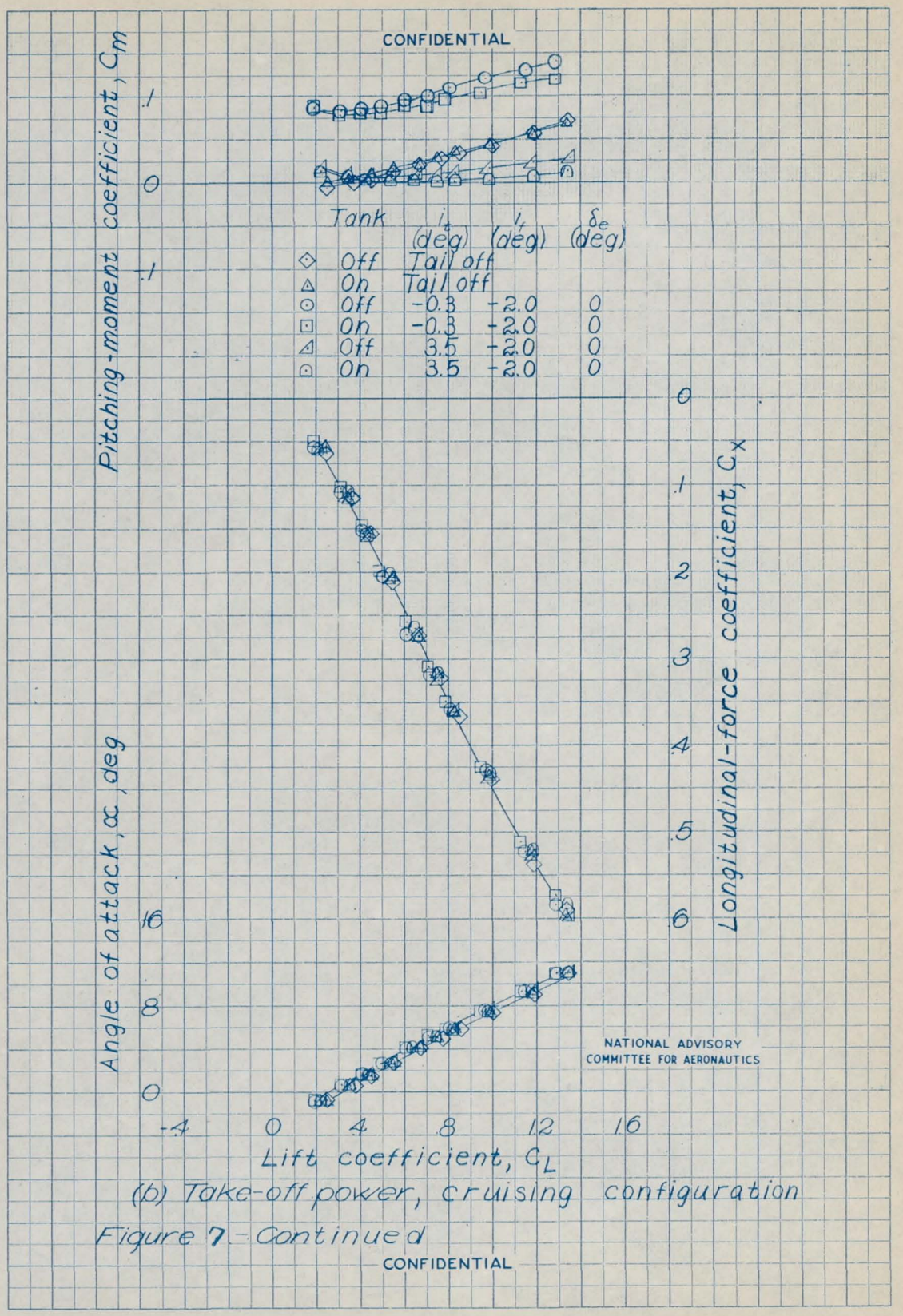

(b) Take-off power, cruising configuration

Figure 7 - Continued

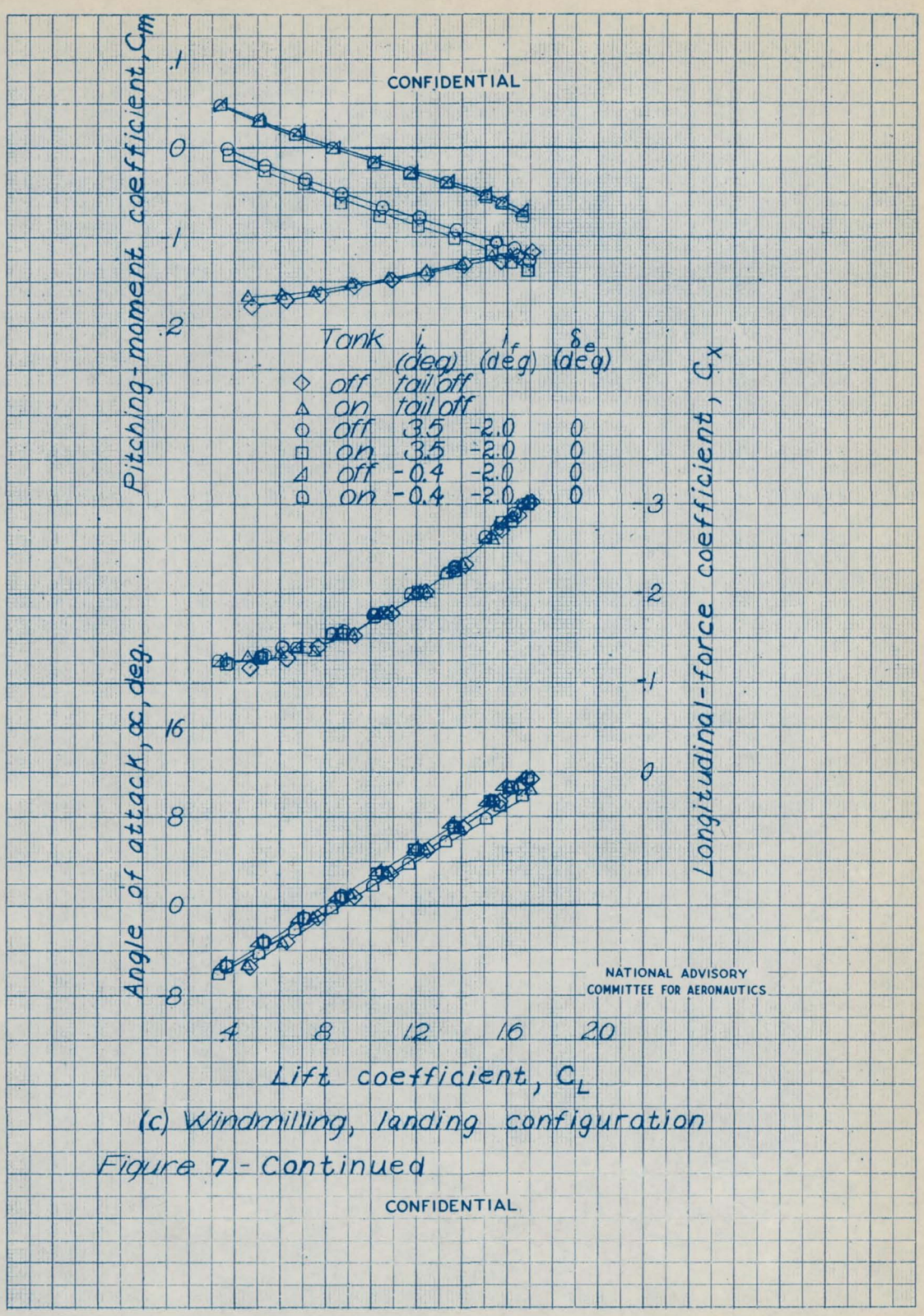

(c) Windmilling, landing configuration

Figure 7.- Continued

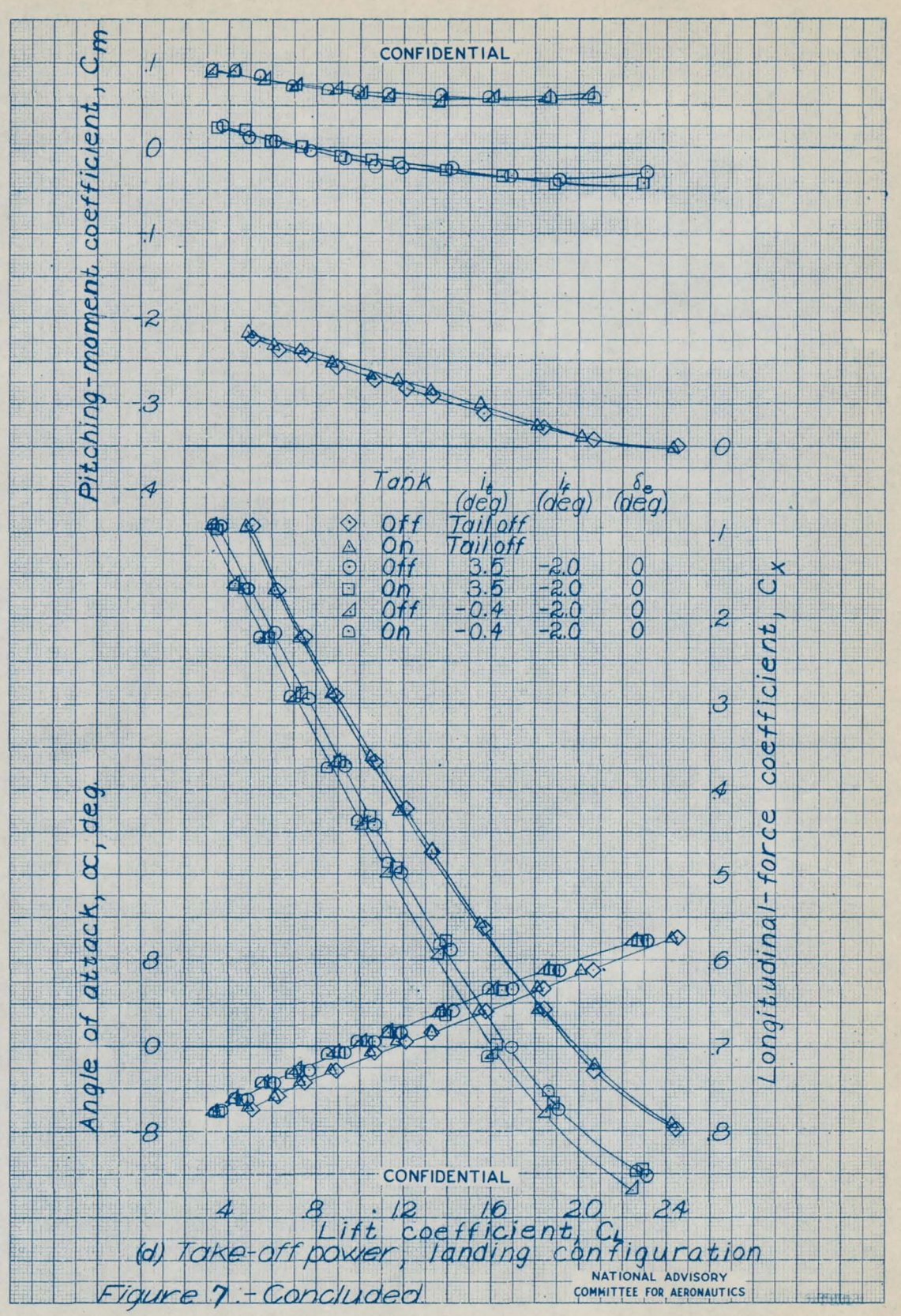

(d) Take-off power, landing configuration

Figure 7.- Concluded

NATIONAL ADVISORY COMMITTEE FOR AERONAUTICS

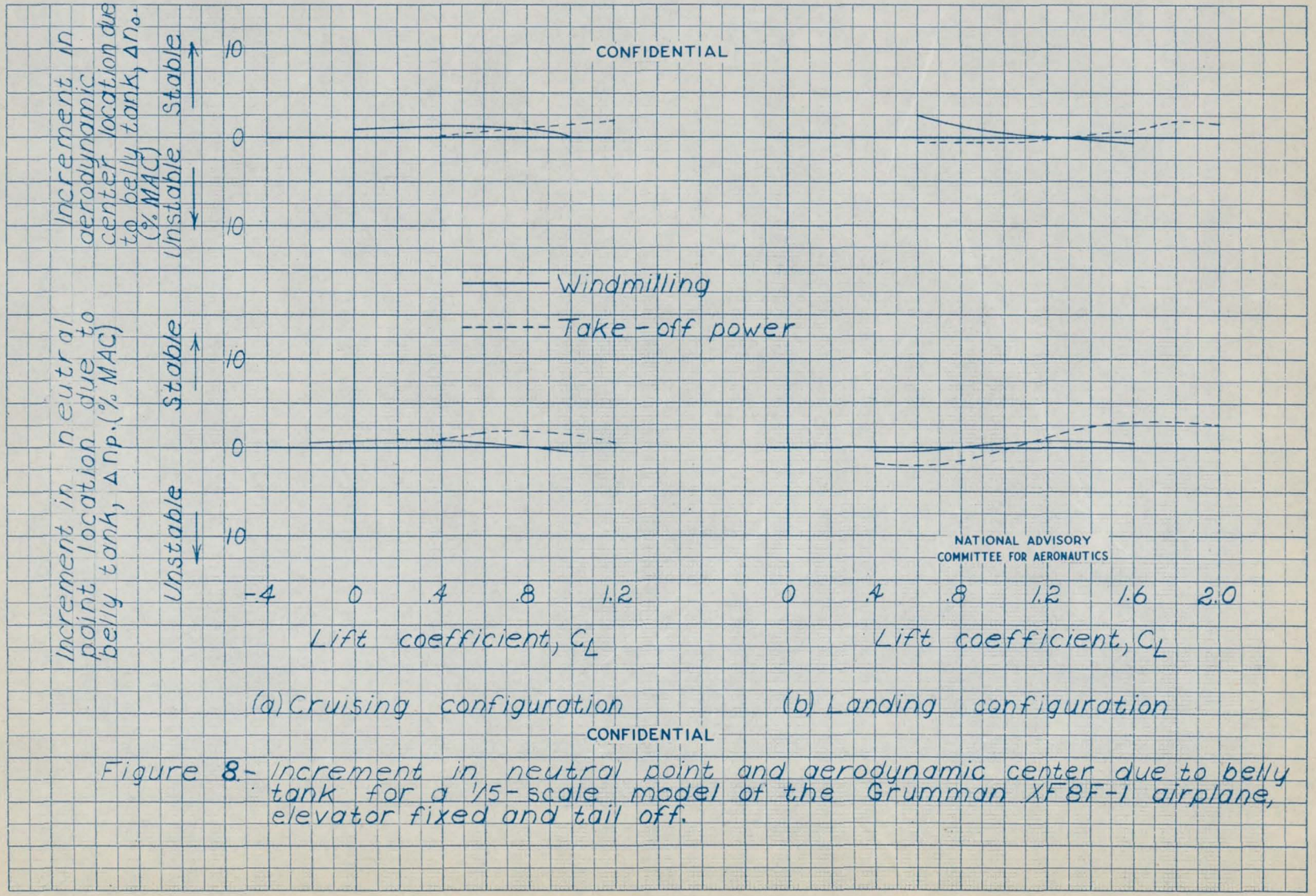

Figure 8.- Increment in neutral point and aerodynamic center due to belly tank for a 1/5-scale model of the Grumman XF8F-1 airplane, elevator fixed and tail off.

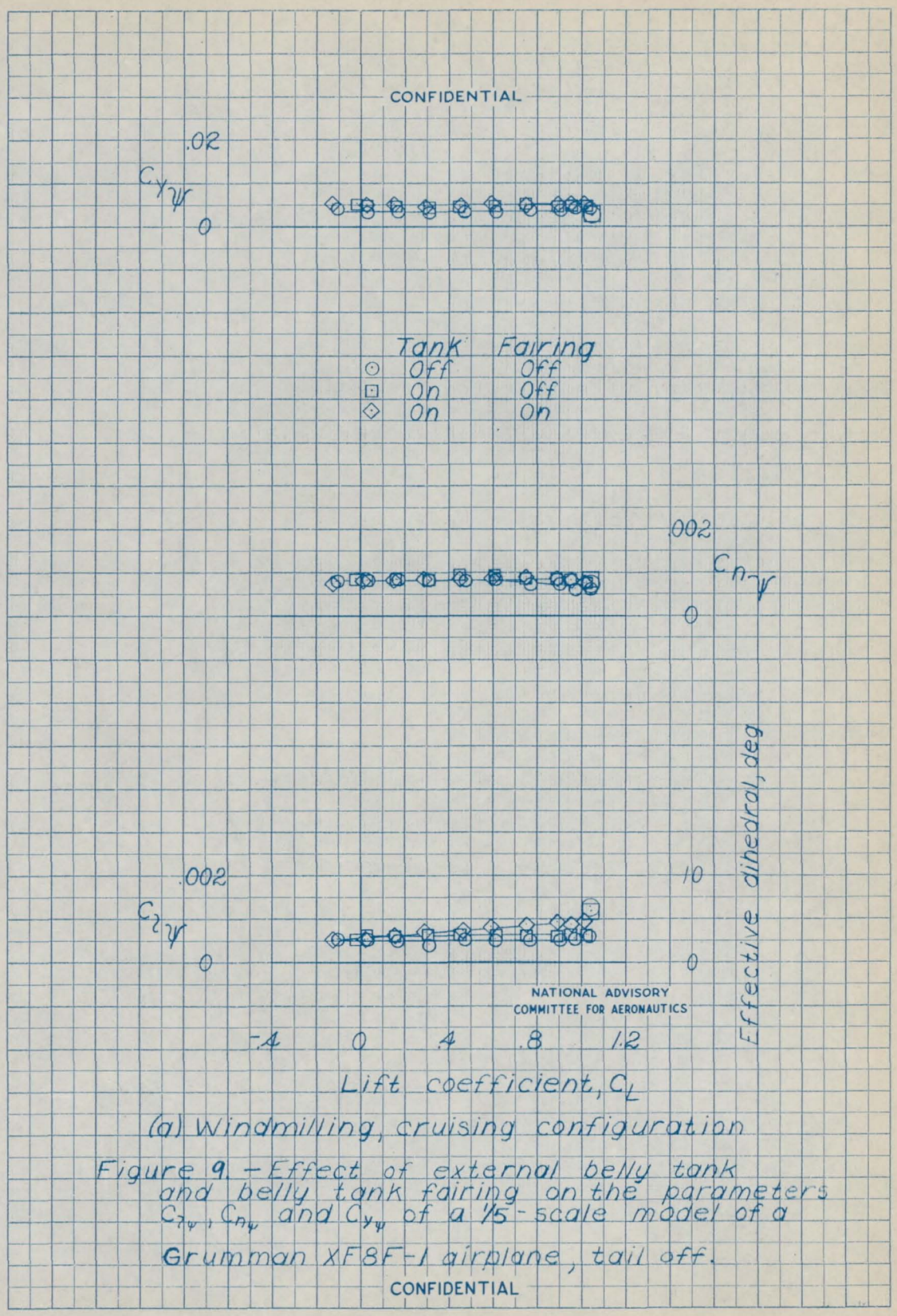

(a) Windmilling, cruising configuration

Figure 9 - Effect of external belly tank and belly tank fairing on the parameters C_{l_ψ}, C_{n_ψ} and C_{Y_ψ} of a 1/5-scale model of a Grumman XF8F-1 airplane, tail off.

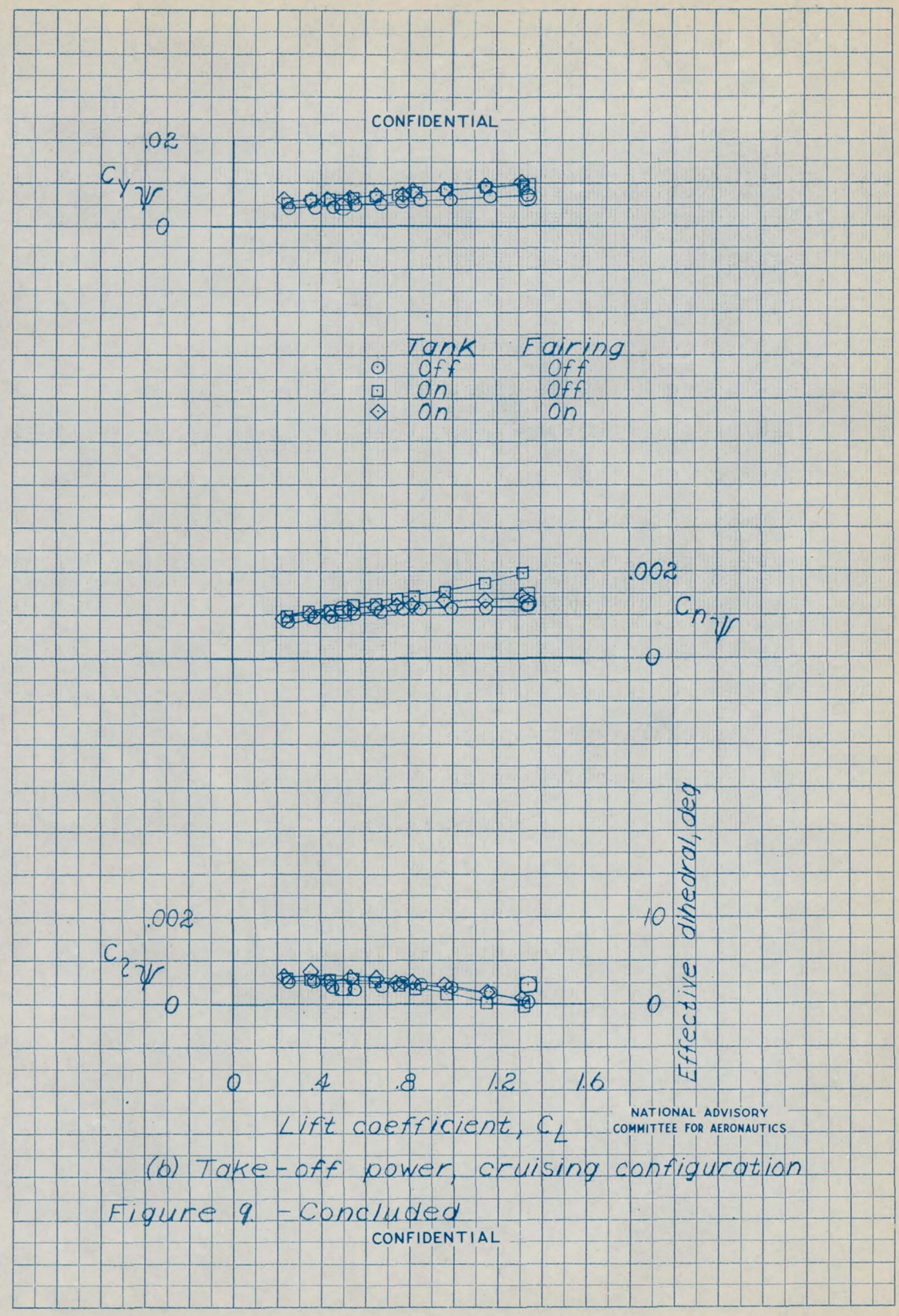

(b) Take-off power, cruising configuration

Figure 9 - Concluded

CONFIDENTIAL

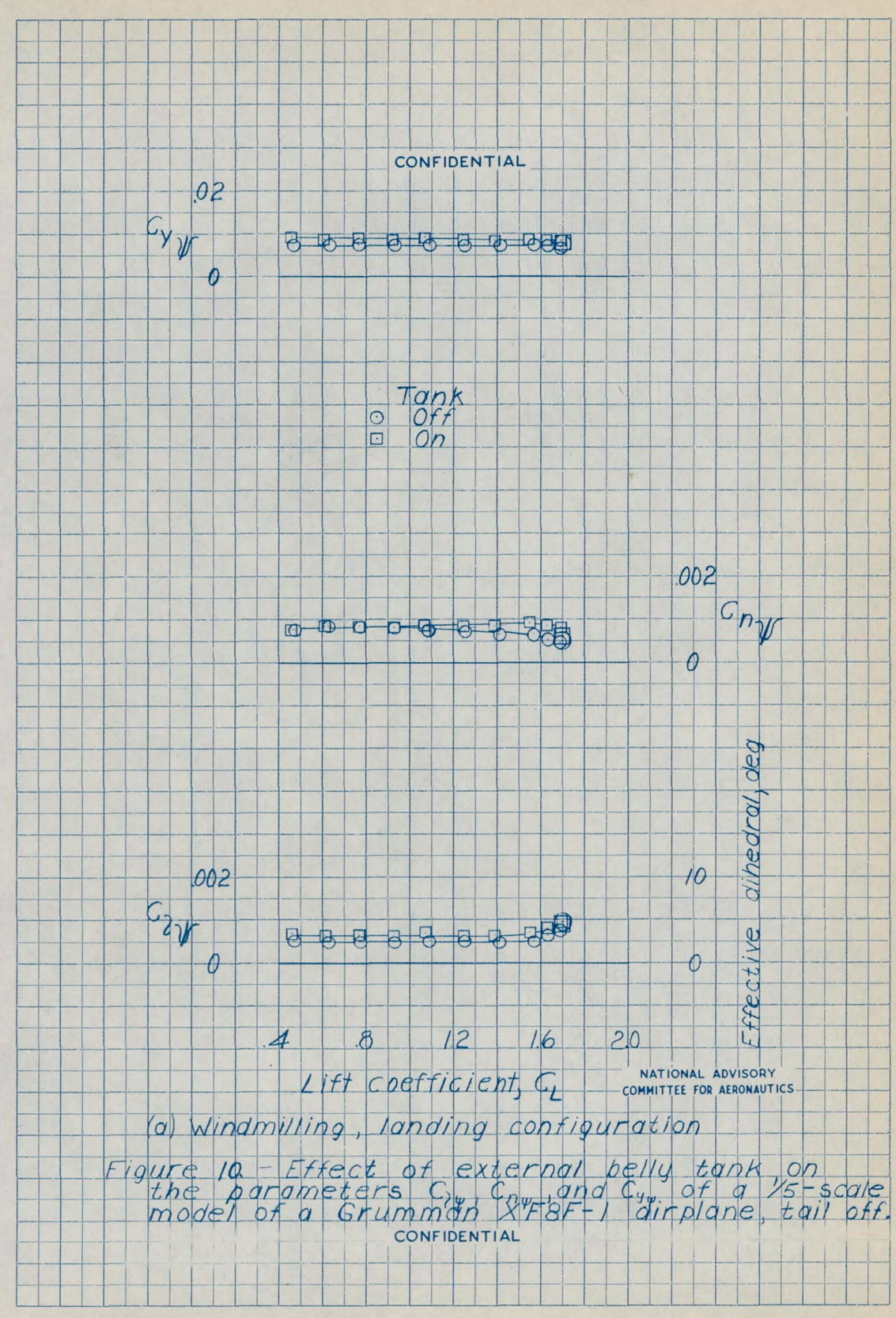

(a) Windmilling, landing configuration

Figure 10 - Effect of external belly tank on the parameters C_{l_Ψ}, C_{n_Ψ}, and C_{Y_Ψ} of a 1/5-scale model of a Grumman XF8F-1 airplane, tail off.

CONFIDENTIAL

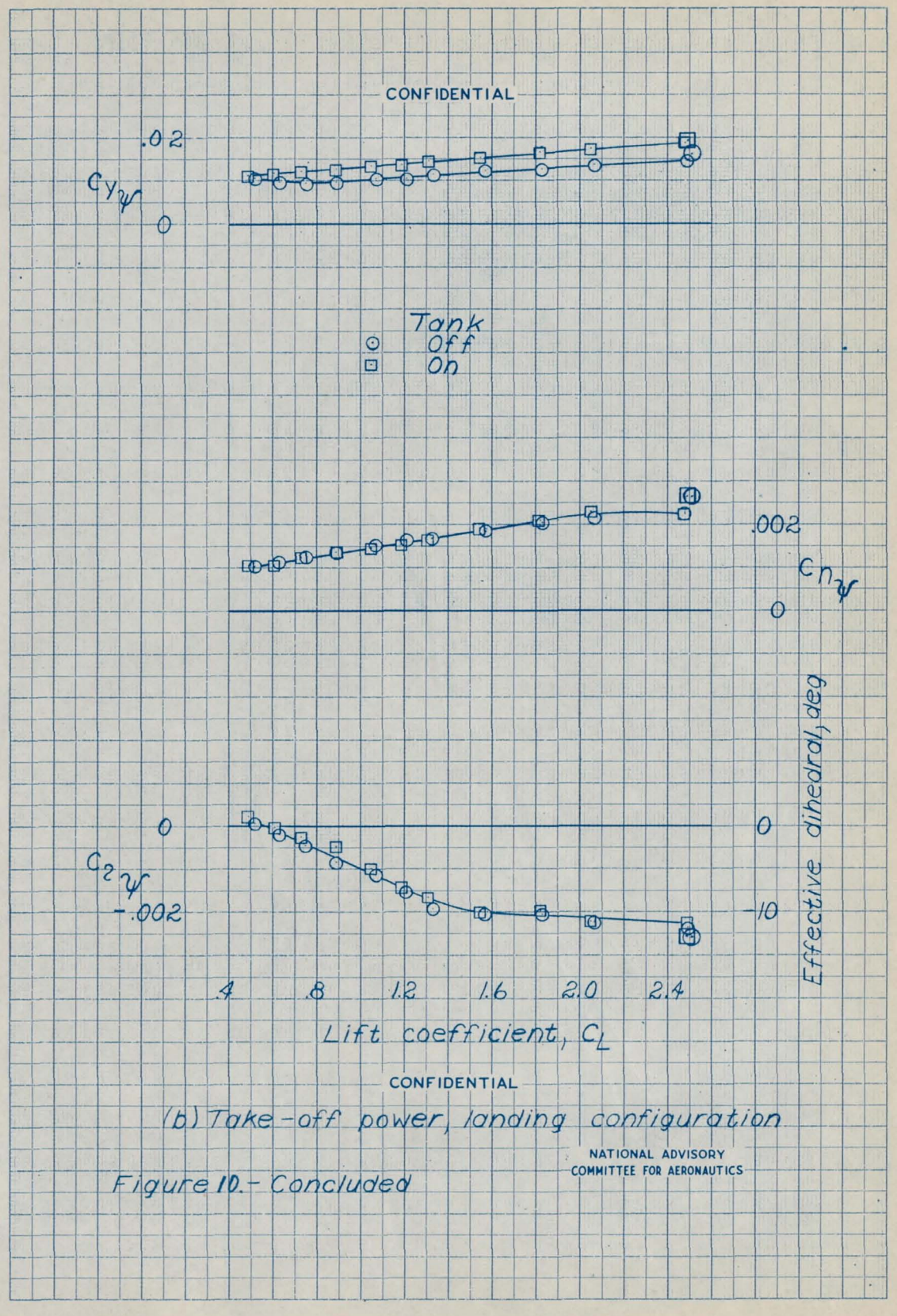

(b) Take-off power, landing configuration

NATIONAL ADVISORY COMMITTEE FOR AERONAUTICS

Figure 10.- Concluded

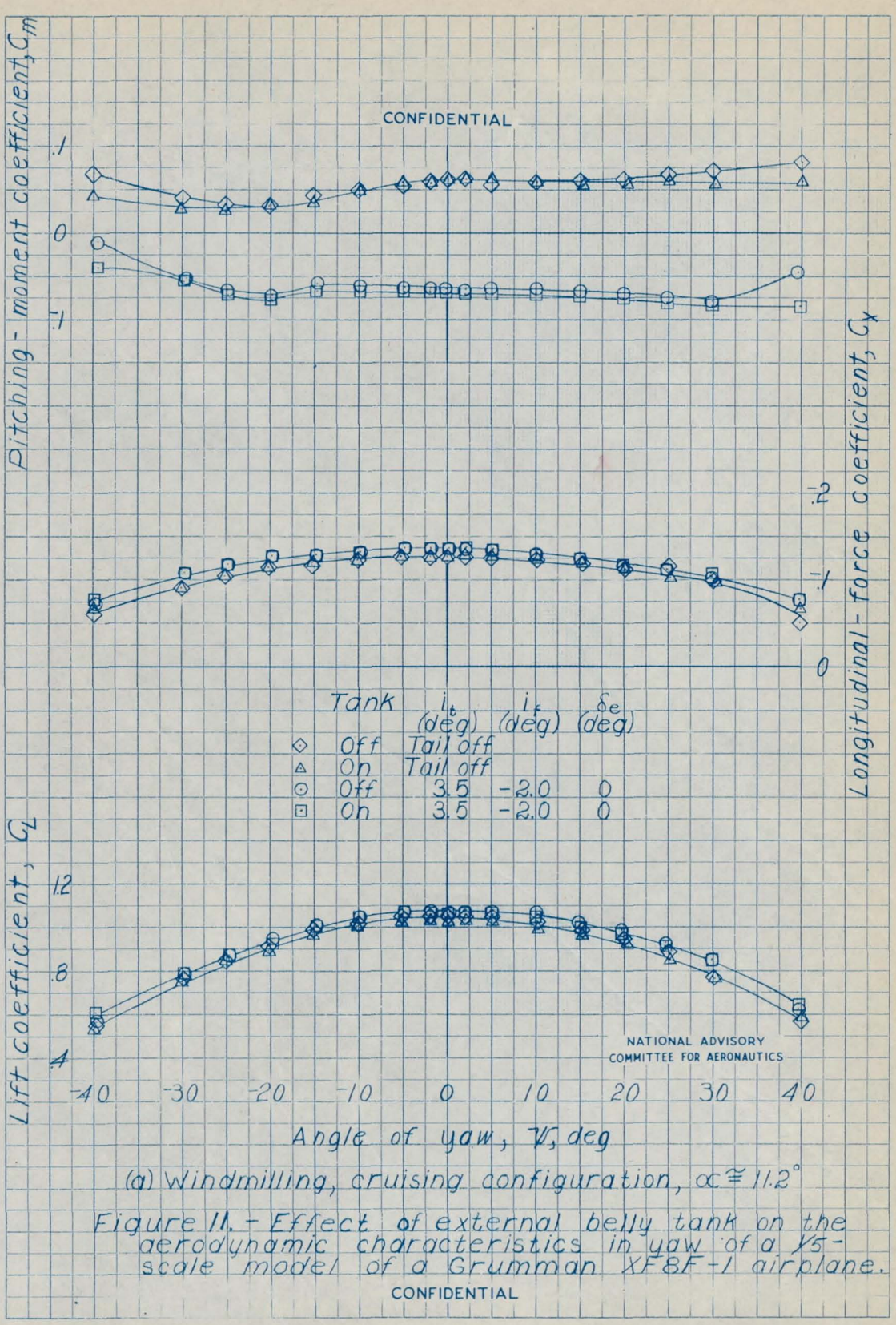

(a) Windmilling, cruising configuration, $\alpha \cong 11.2°$

Figure 11. - Effect of external belly tank on the aerodynamic characteristics in yaw of a 1/5-scale model of a Grumman XF8F-1 airplane.

CONFIDENTIAL

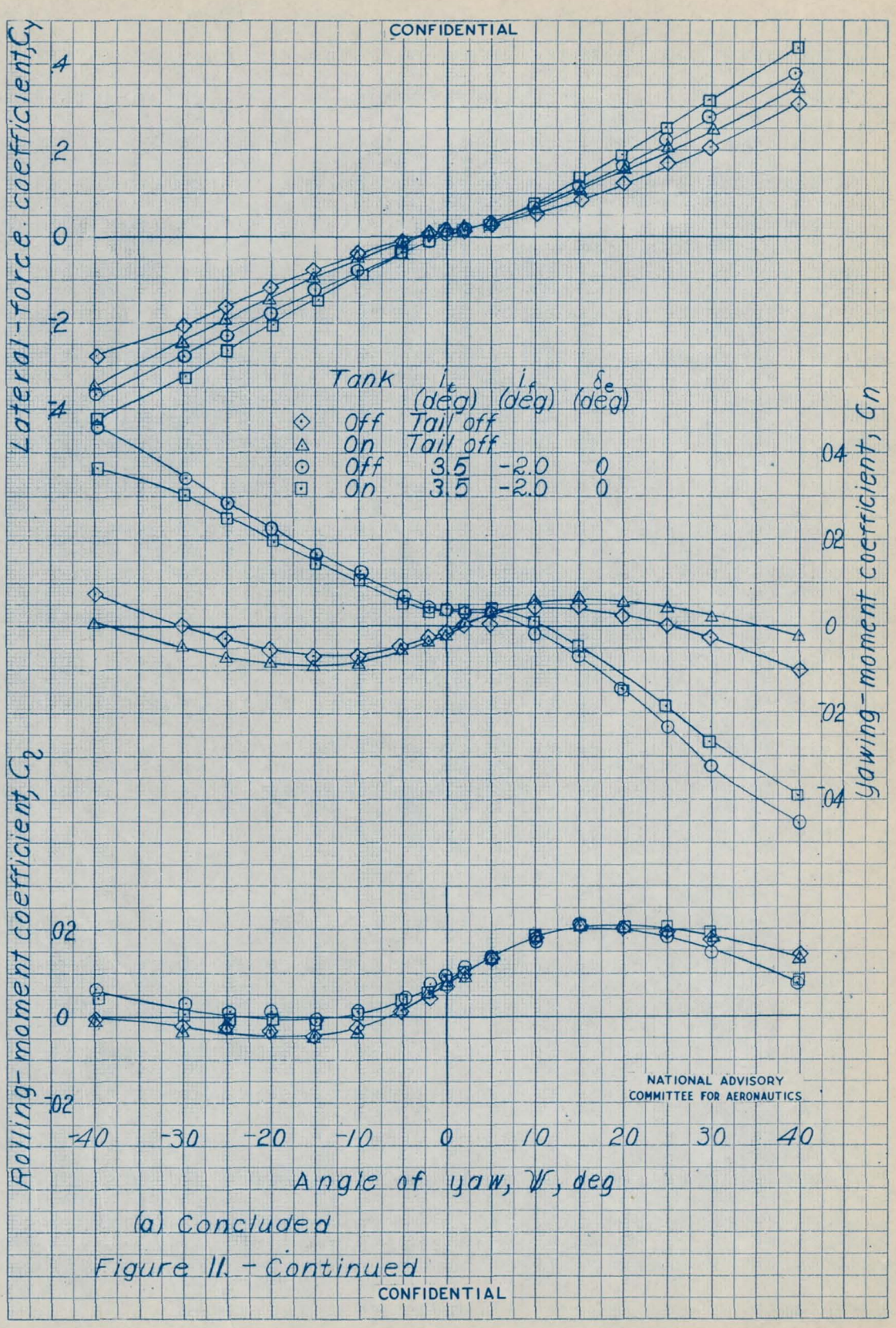

(a) Concluded

Figure 11. - Continued

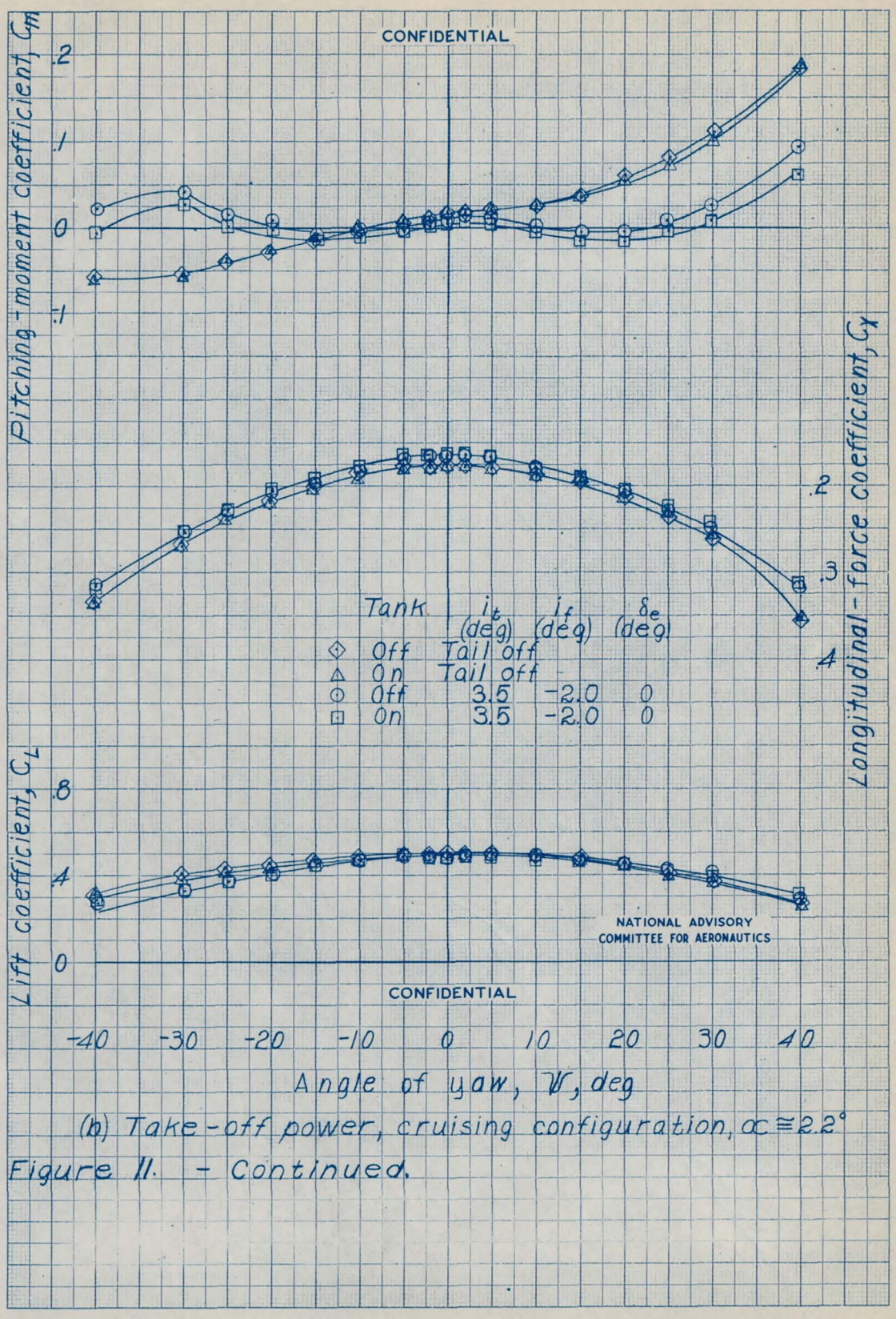

(b) Take-off power, cruising configuration, $\alpha \cong 2.2°$

Figure 11. - Continued.

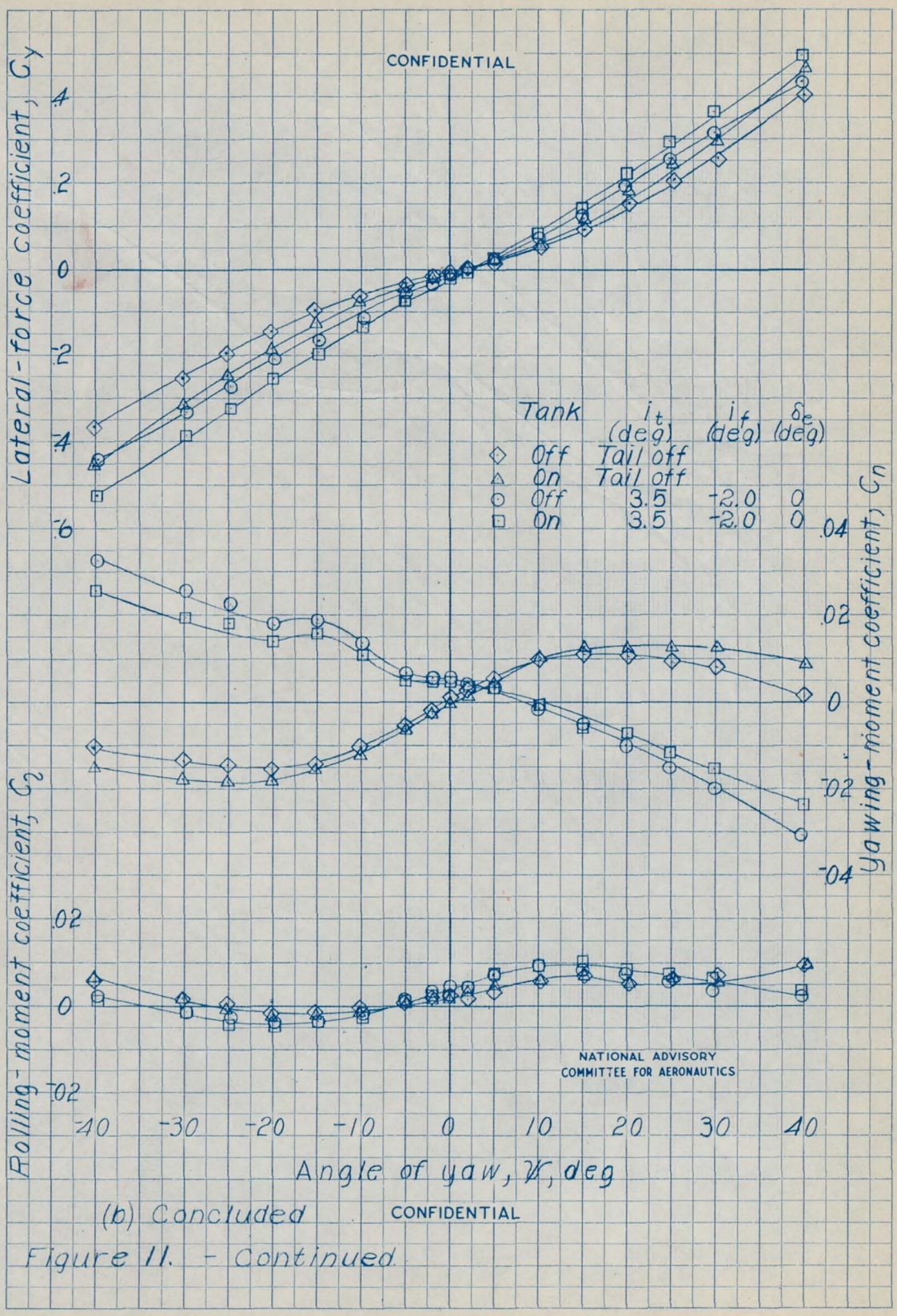

(b) Concluded

Figure 11. - Continued

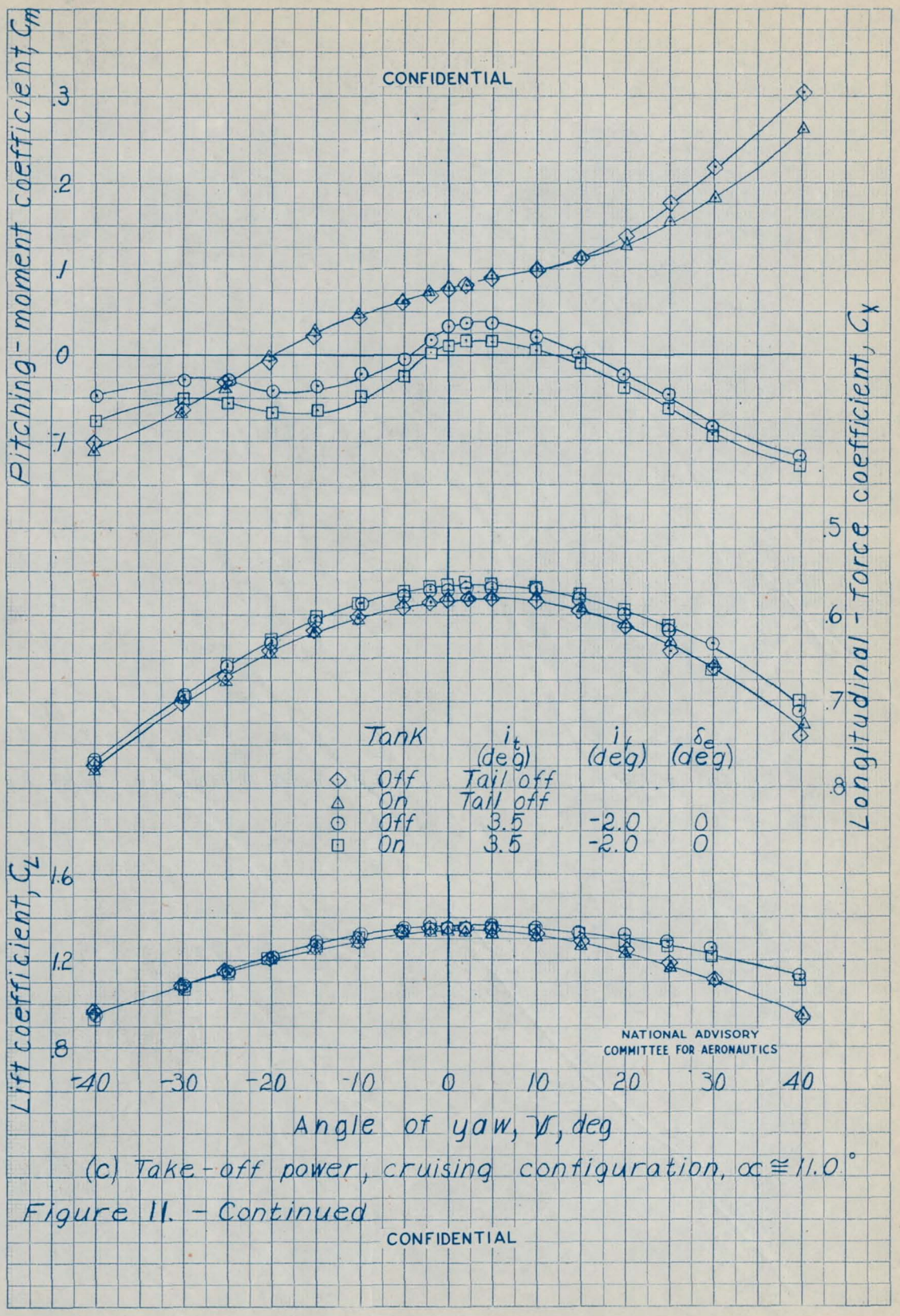

(c) Take-off power, cruising configuration, $\alpha \cong 11.0°$

Figure 11. - Continued

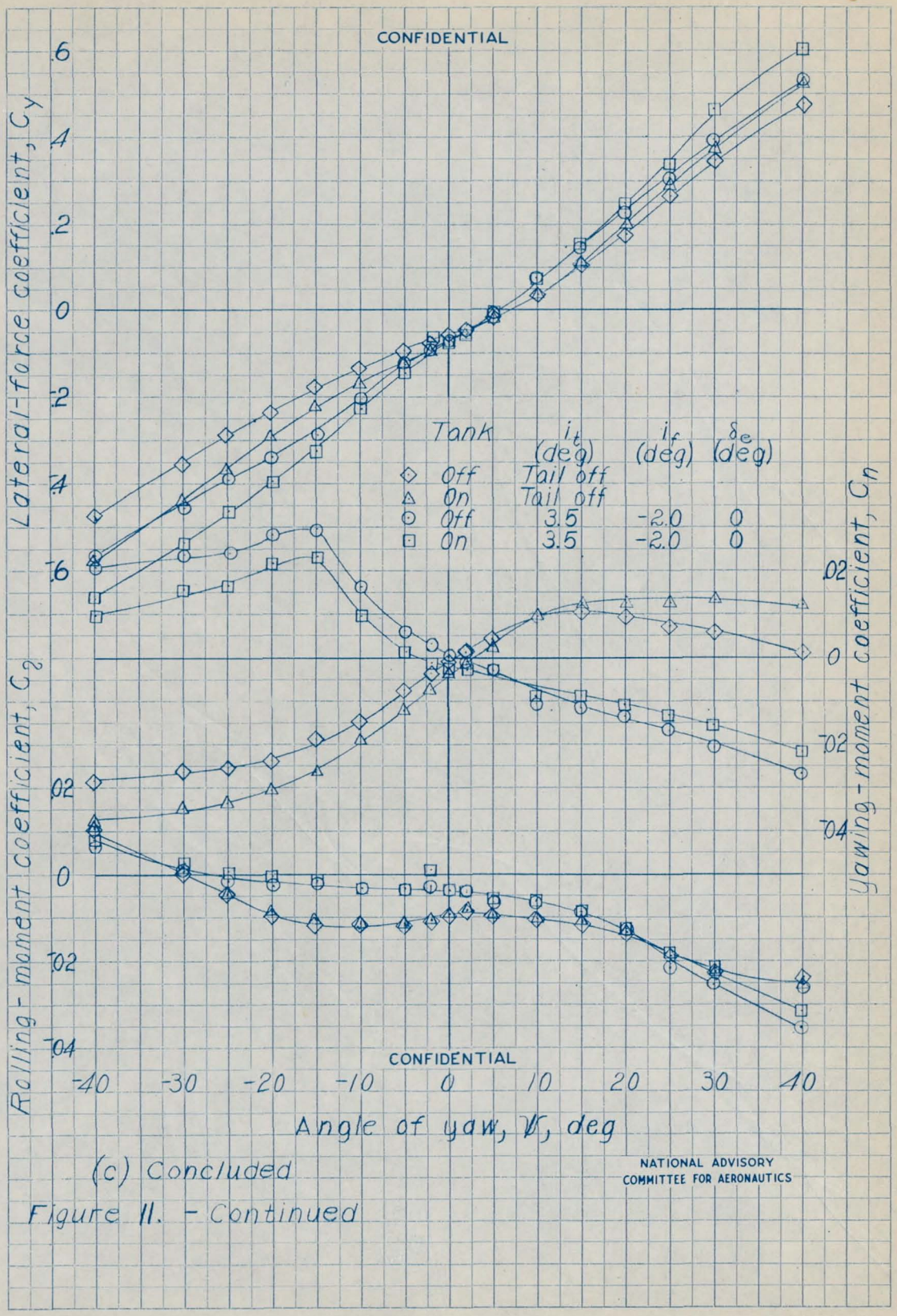

(c) Concluded

Figure 11. - Continued

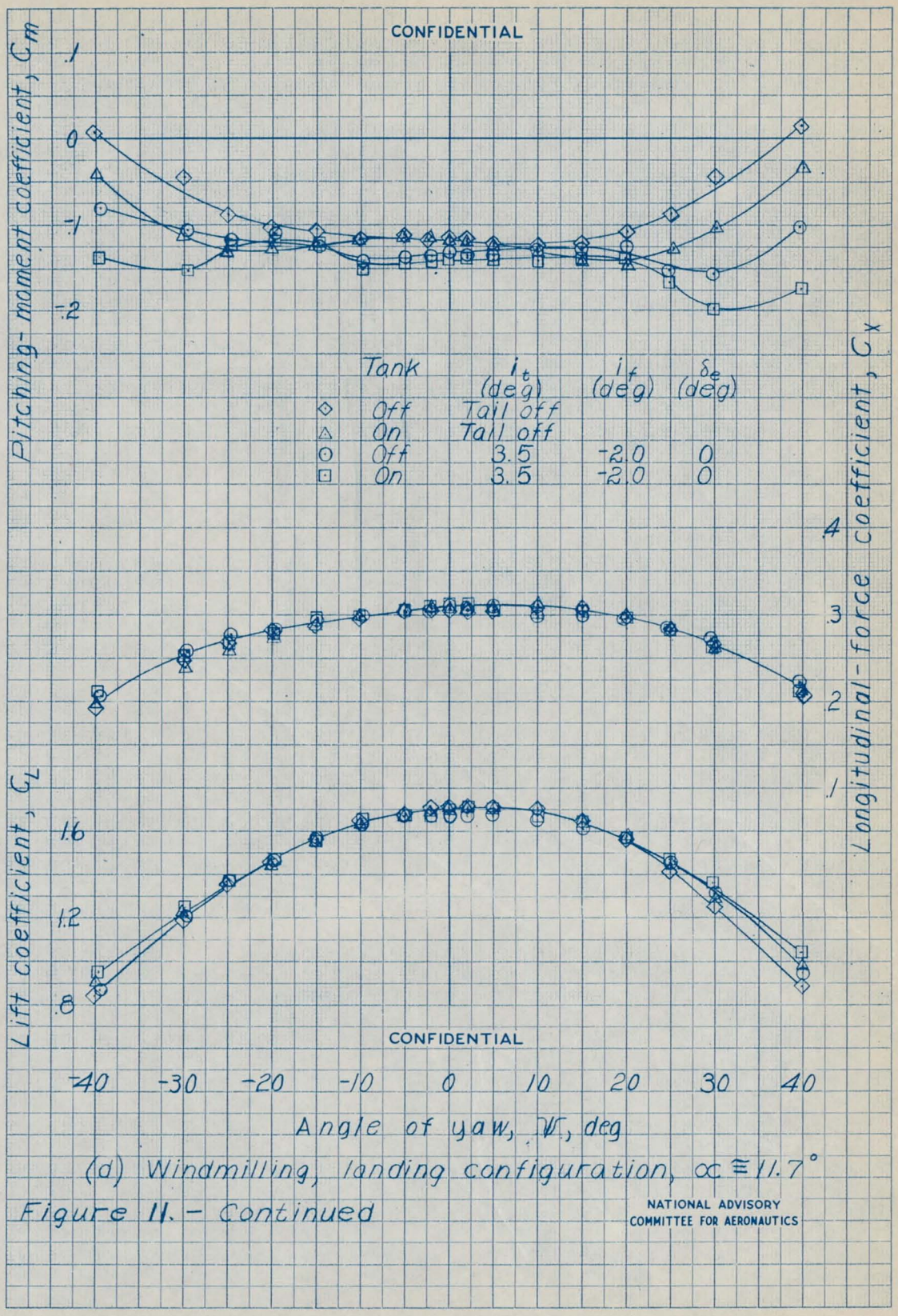

(d) Windmilling, landing configuration, $\alpha \equiv 11.7°$

Figure 11. – Continued

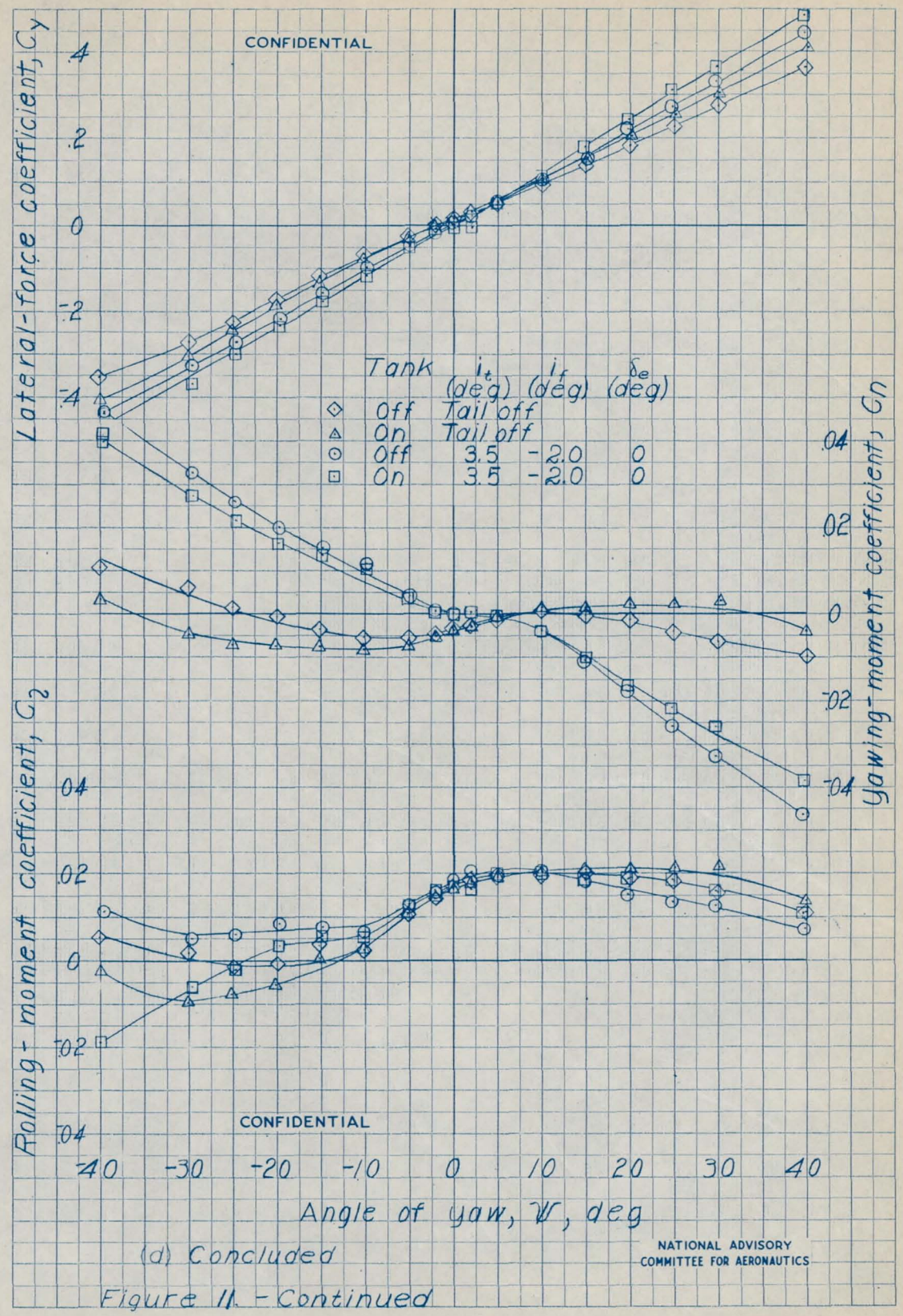

NATIONAL ADVISORY COMMITTEE FOR AERONAUTICS

(d) Concluded

Figure 11. - Continued

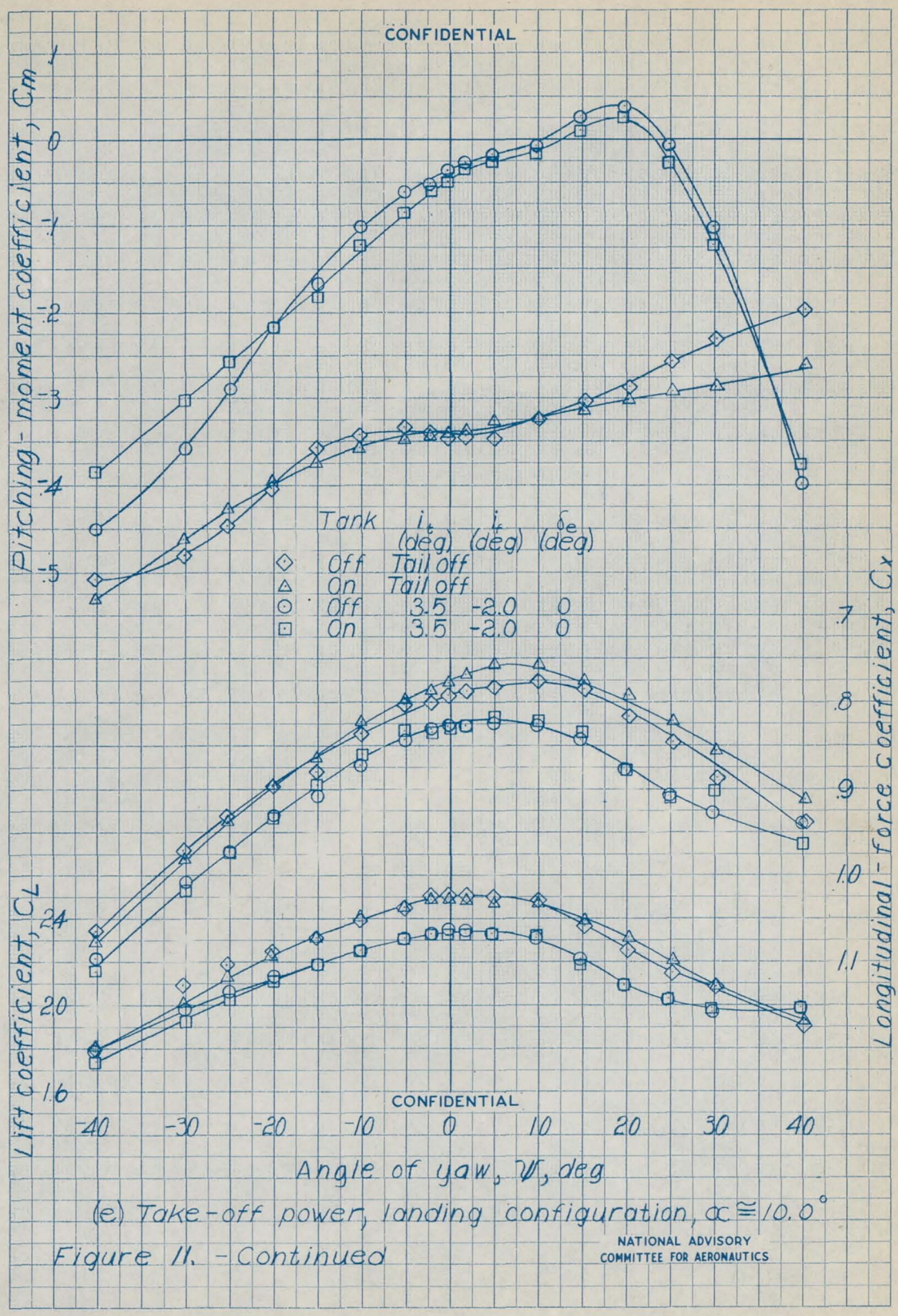

(e) Take-off power, landing configuration, $\alpha \cong 10.0°$

Figure 11. - Continued

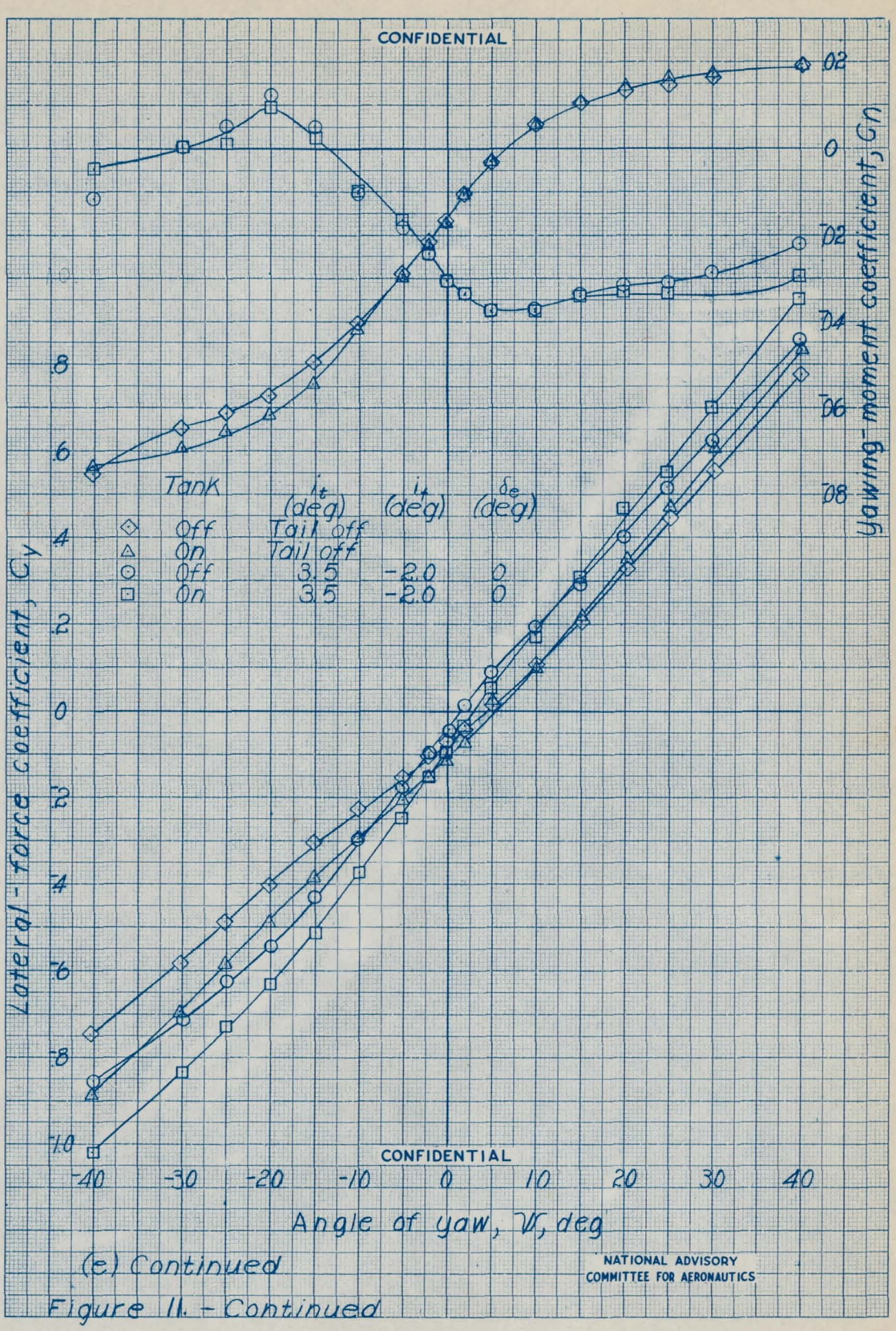

(e) Continued

Figure 11. - Continued

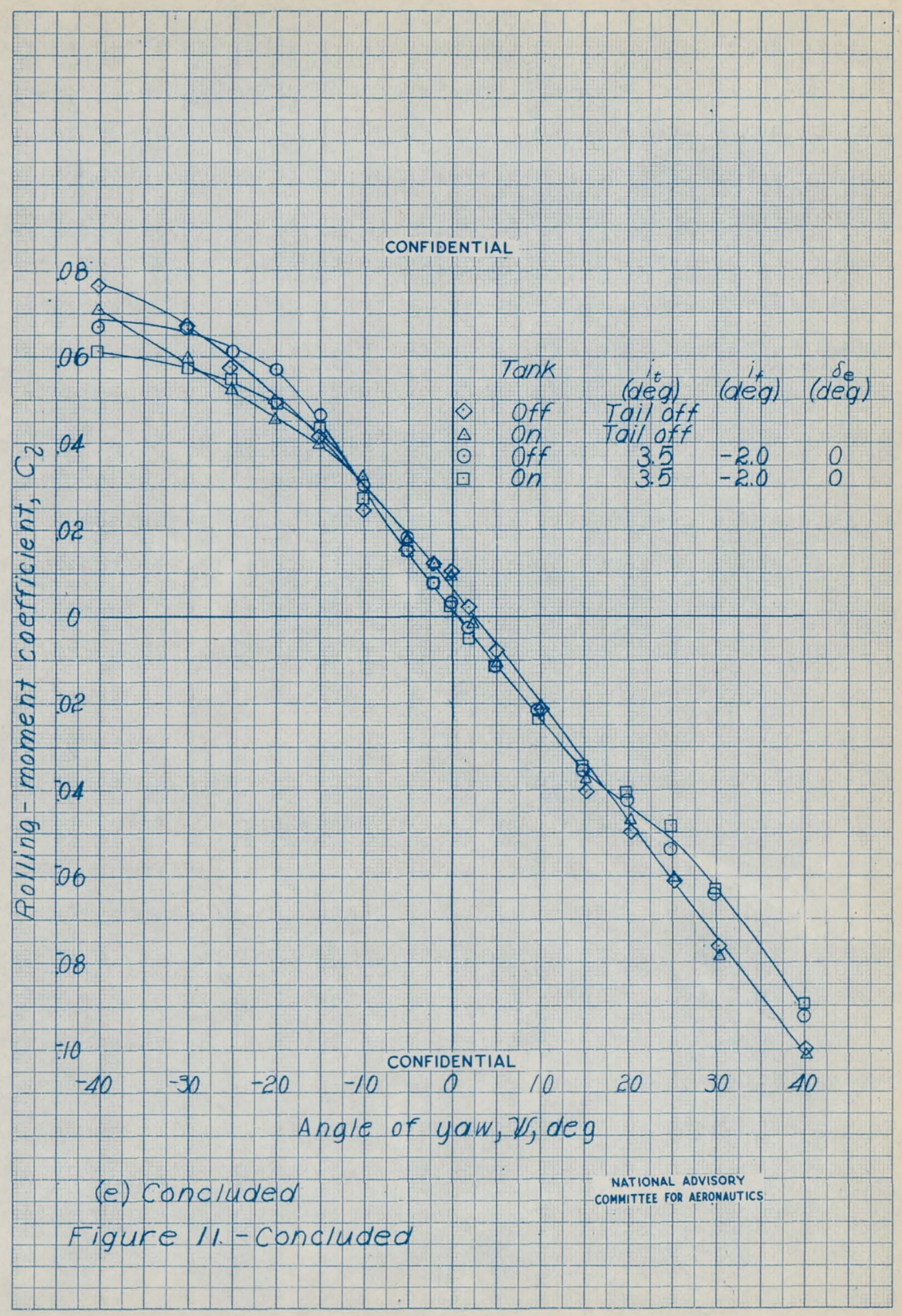

(e) Concluded

Figure 11.-Concluded

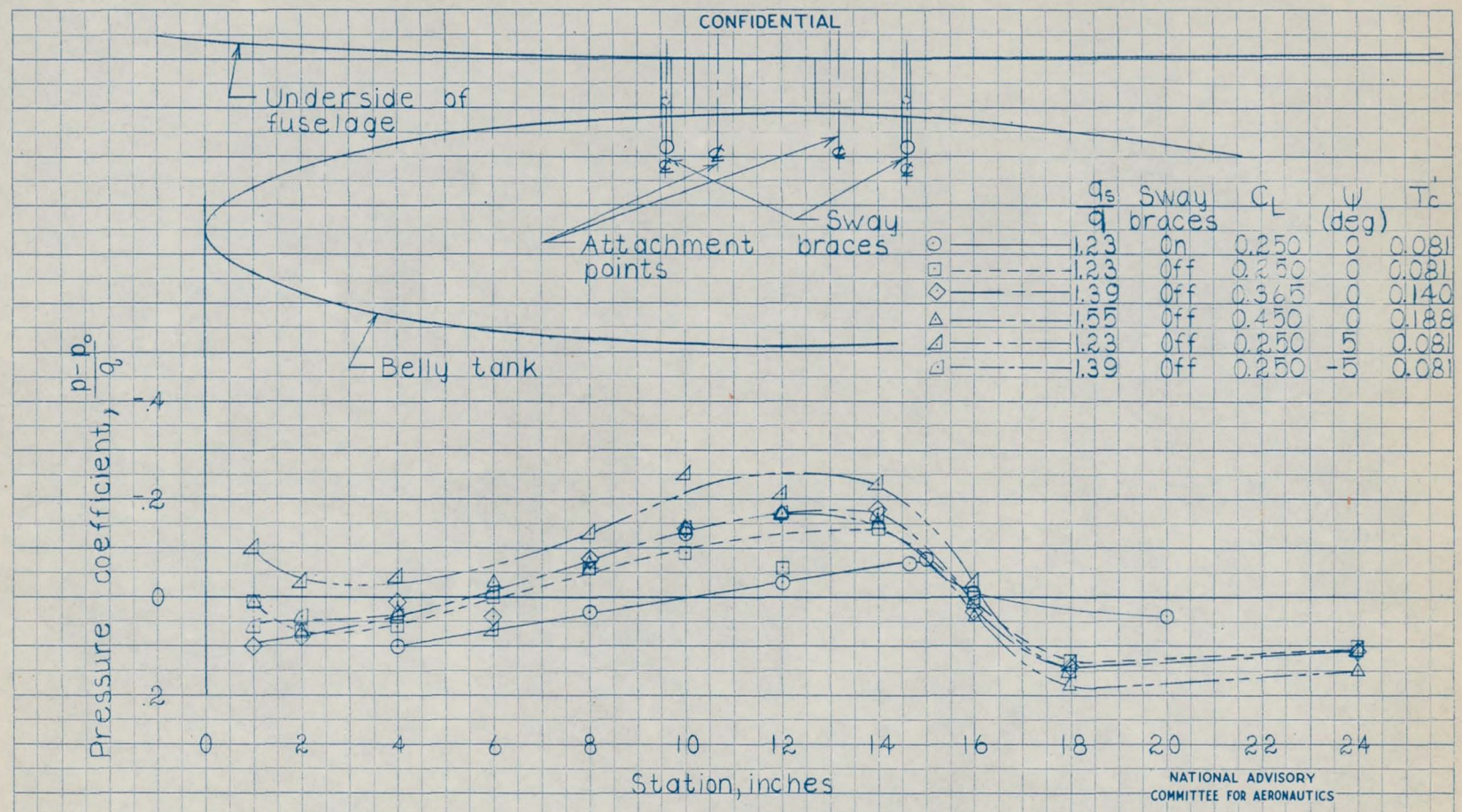

(a) Pressure tube no. 1

Figure 12.- Effect of sway braces, lift coefficient, and angle of yaw on the pressure coefficient on an external belly tank mounted on a 1/5-scale model of a Grumman XF8F-1 airplane. Take-off power (2100 hp at 2800 rpm), cruising condition; tail off.

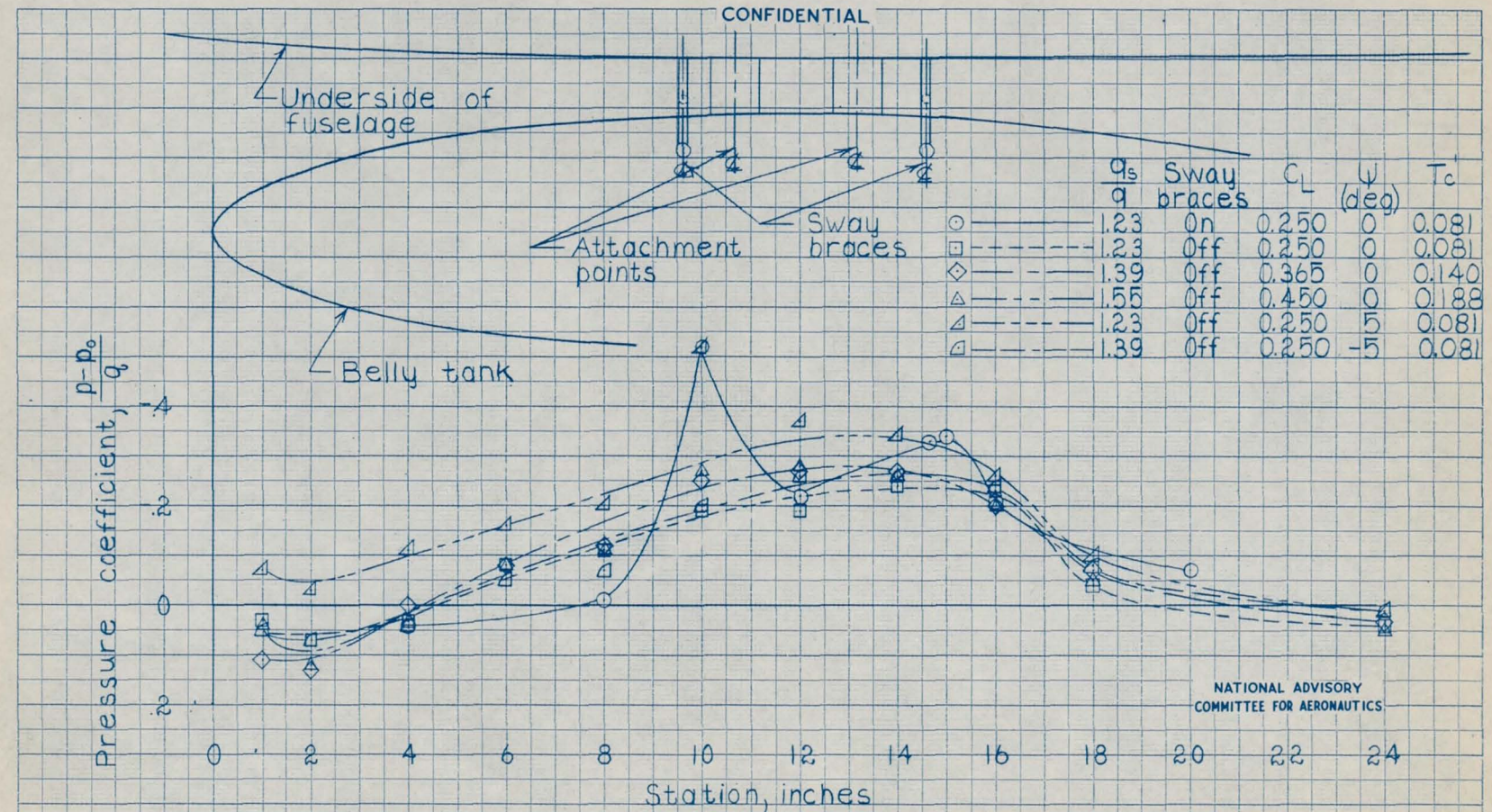

(b) Pressure tube no. 2

Figure 12. - Continued

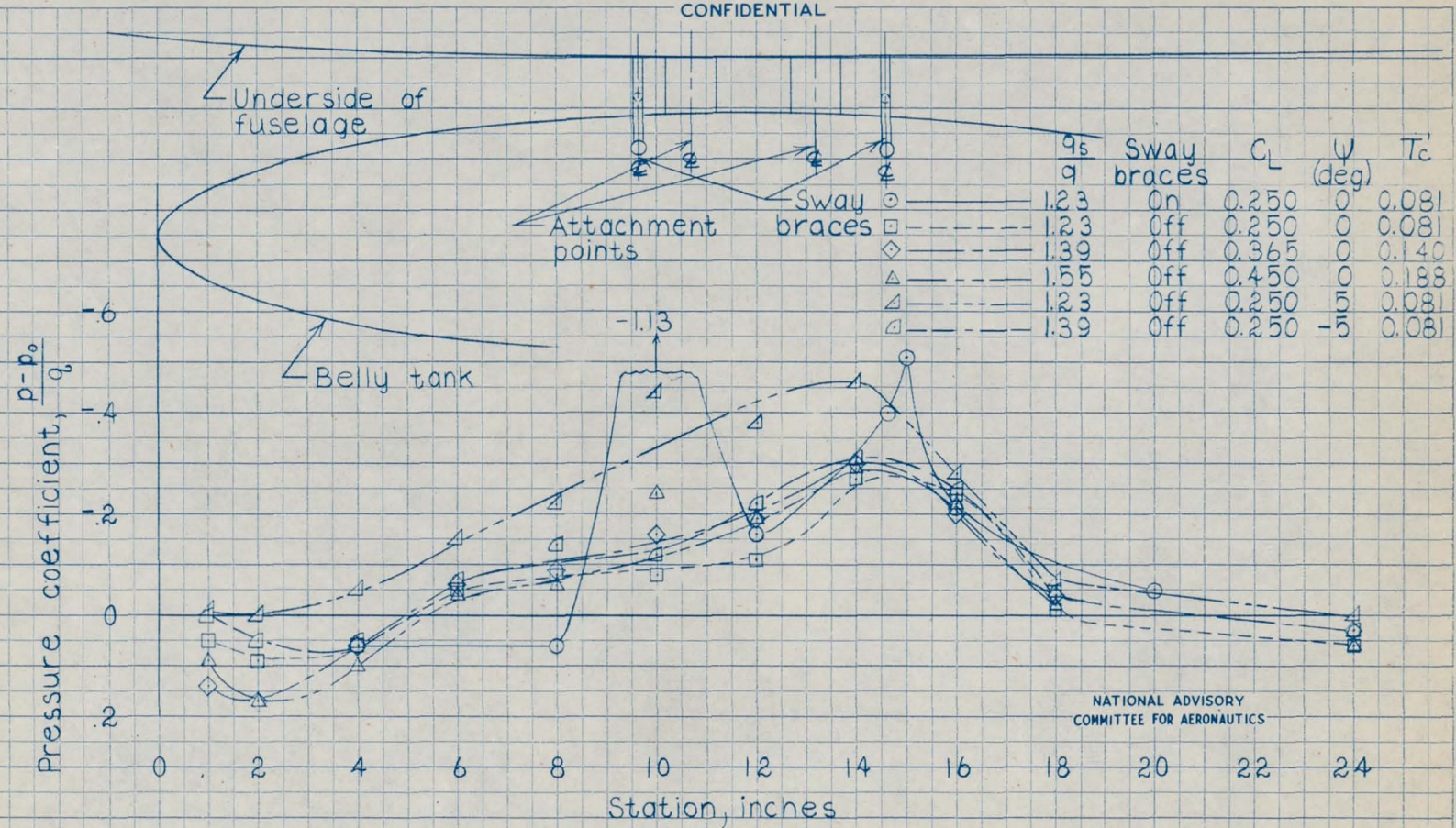

(c) Pressure tube no. 3

Figure 12. - Continued

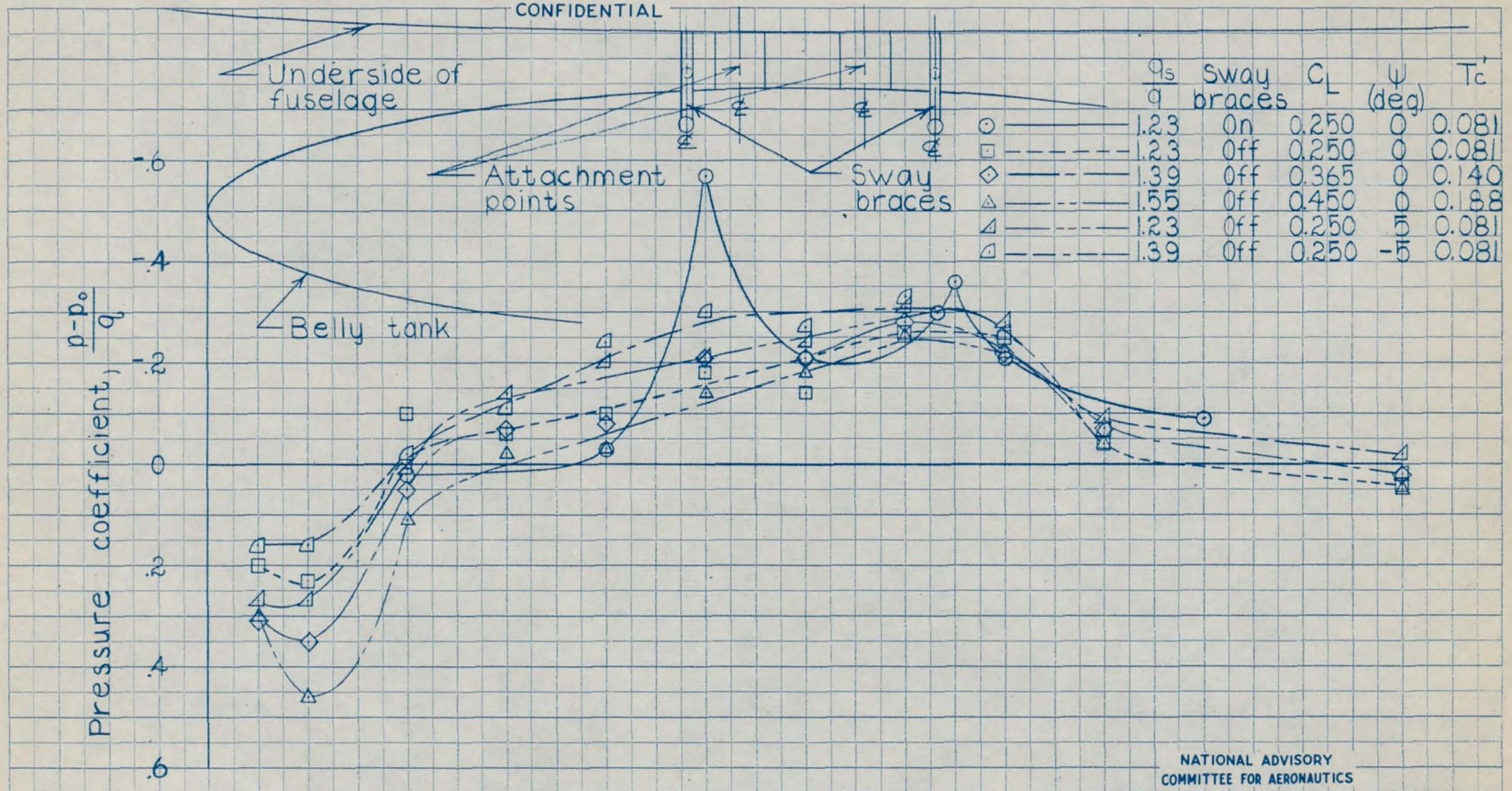

(d) Pressure tube no. 4

Figure 12.- Continued

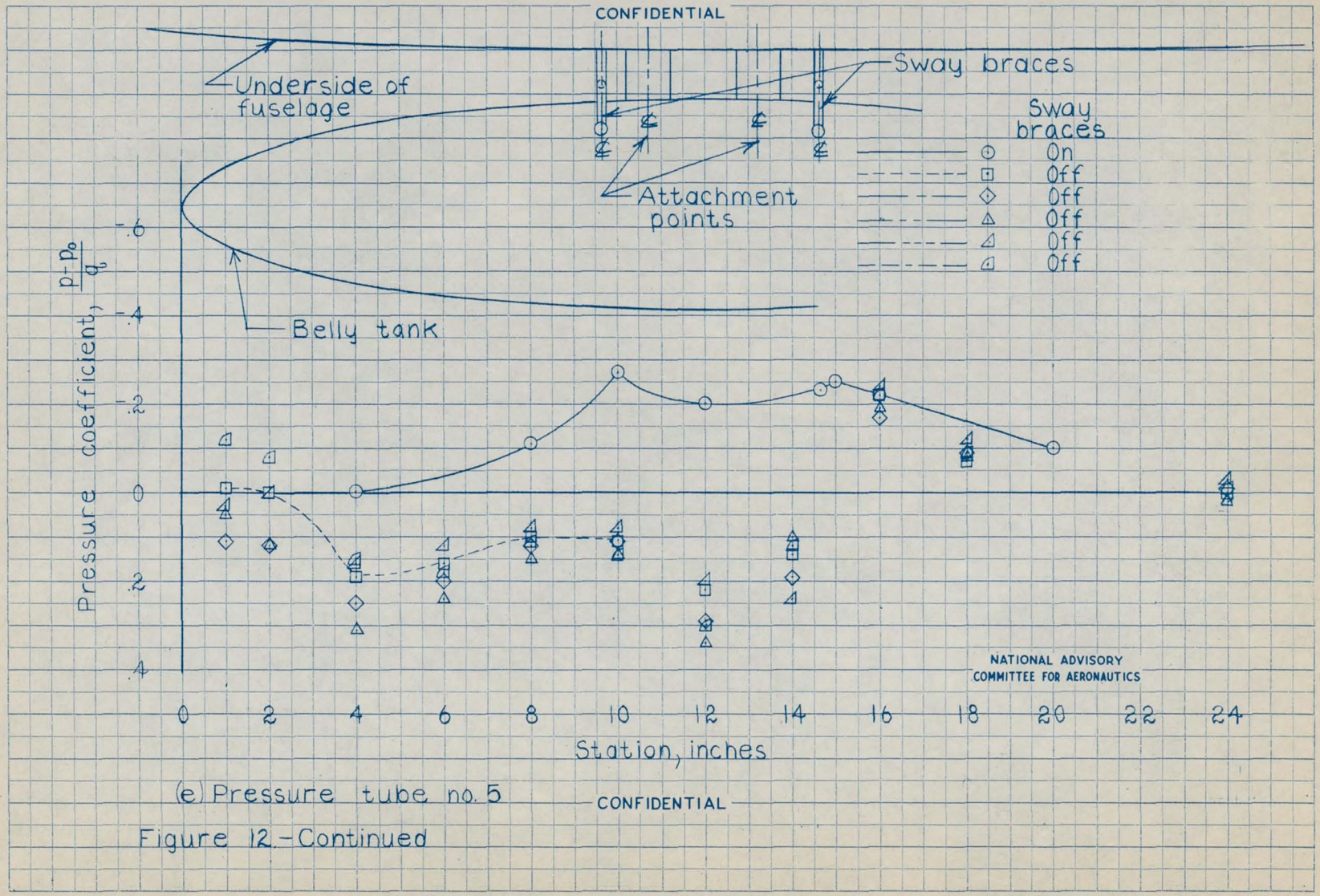

(e) Pressure tube no. 5

Figure 12.-Continued

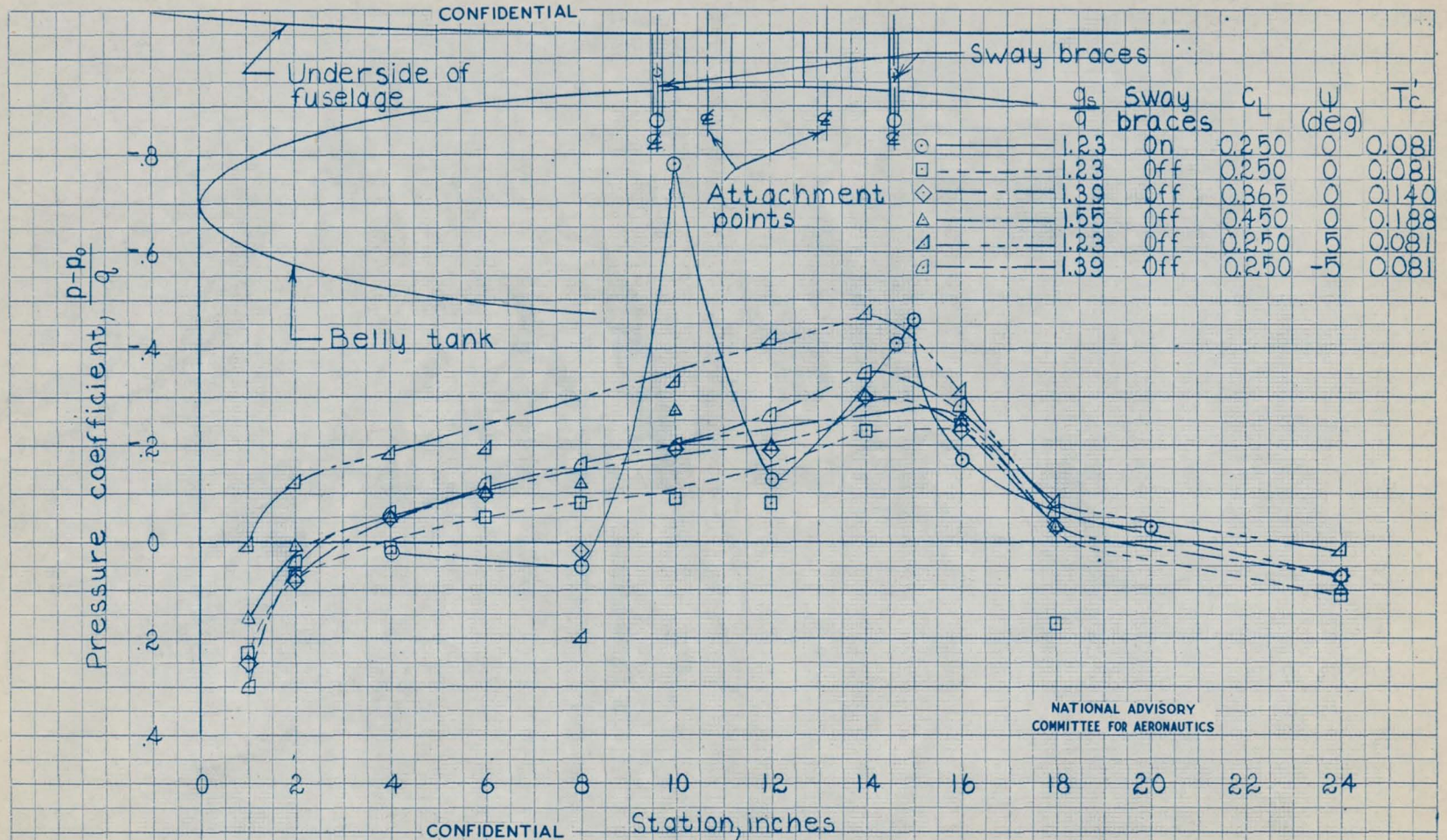

CONFIDENTIAL

(f) Pressure tube no. 6

Figure 12.- Continued

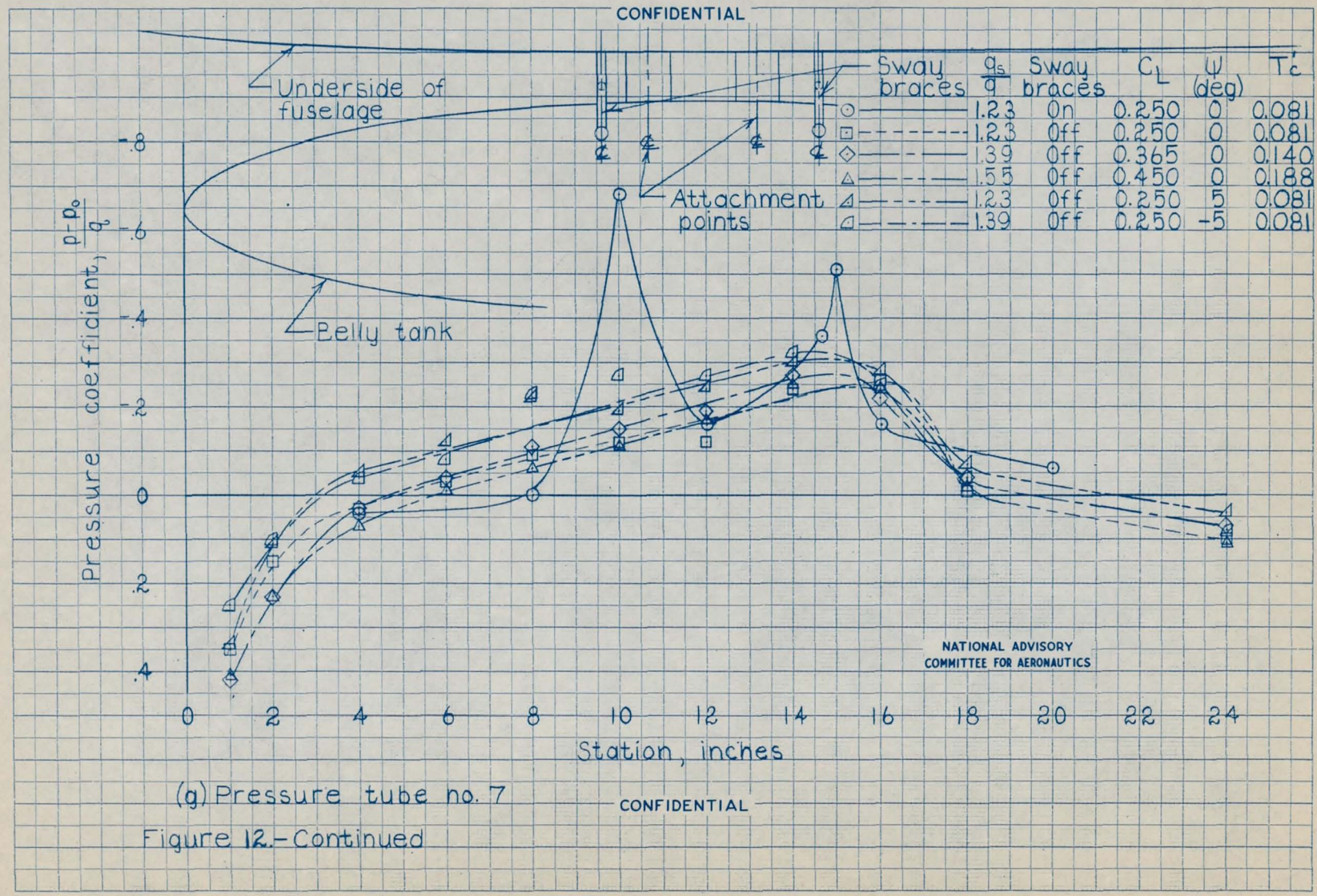

(g) Pressure tube no. 7

Figure 12.- Continued

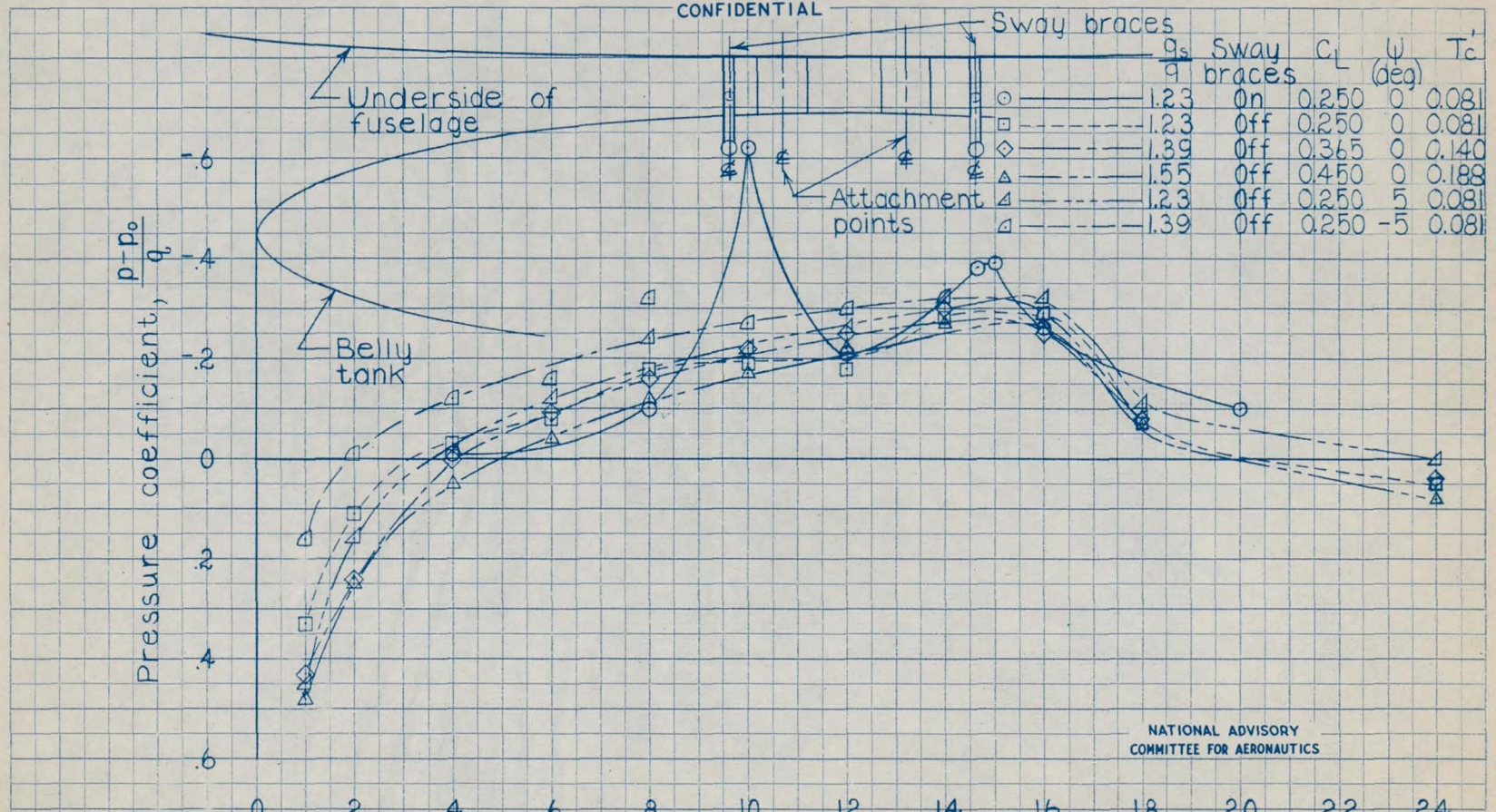

(h) Pressure tube no. 8 CONFIDENTIAL

Figure 12.- Continued

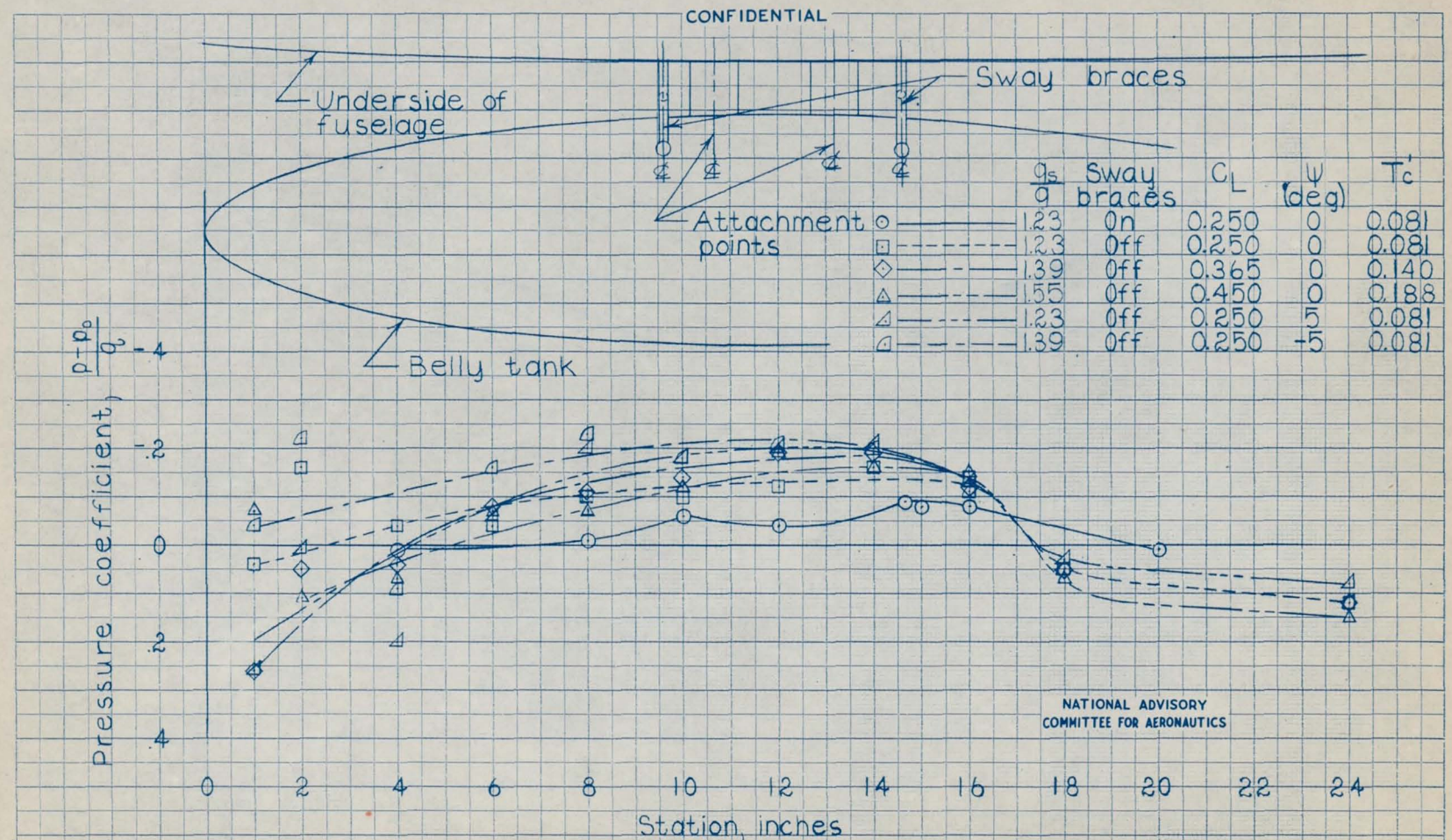

(i) Pressure tube no. 9

CONFIDENTIAL

Figure 12.–Continued

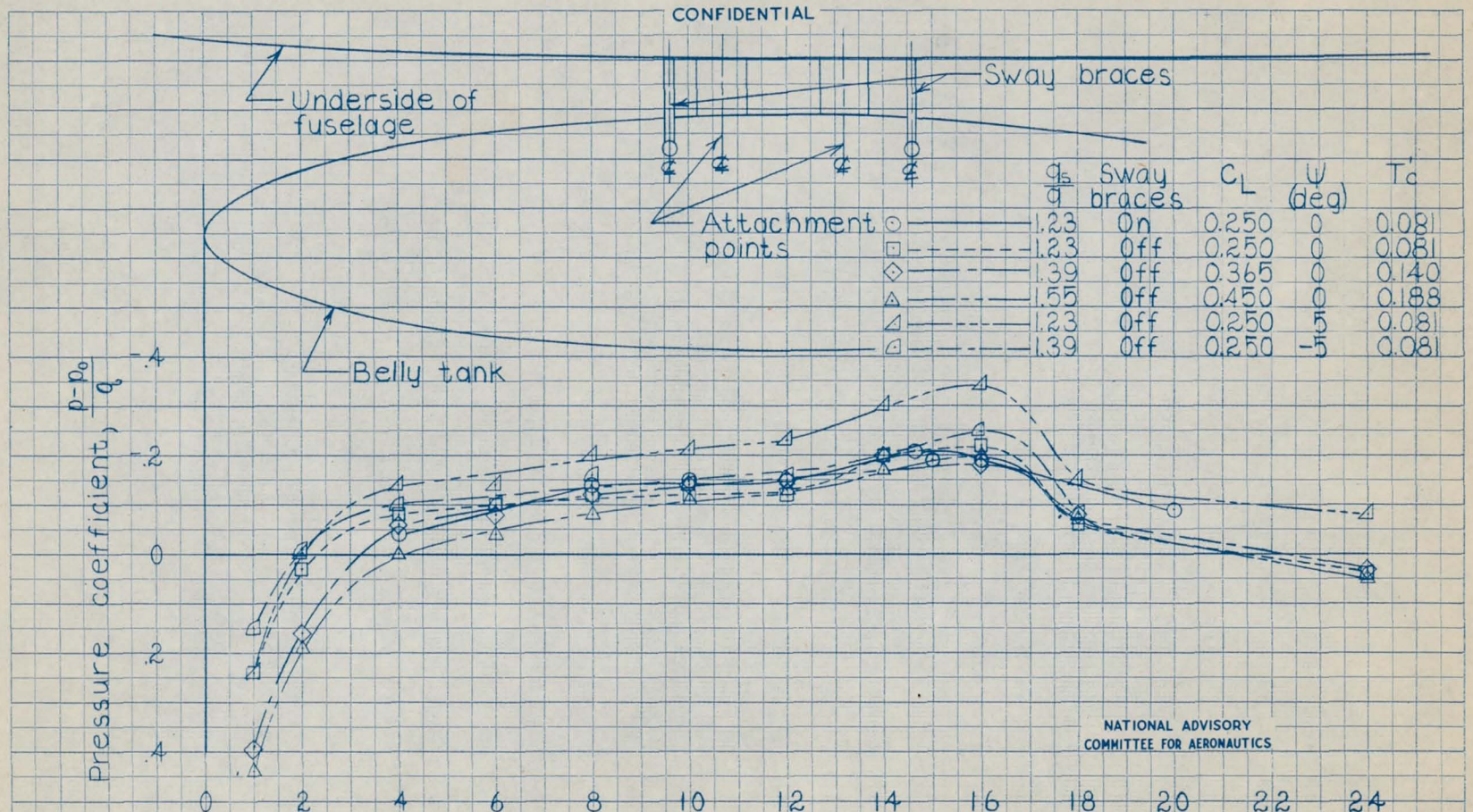

(j) Pressure tube no. 10

Figure 12.- Continued

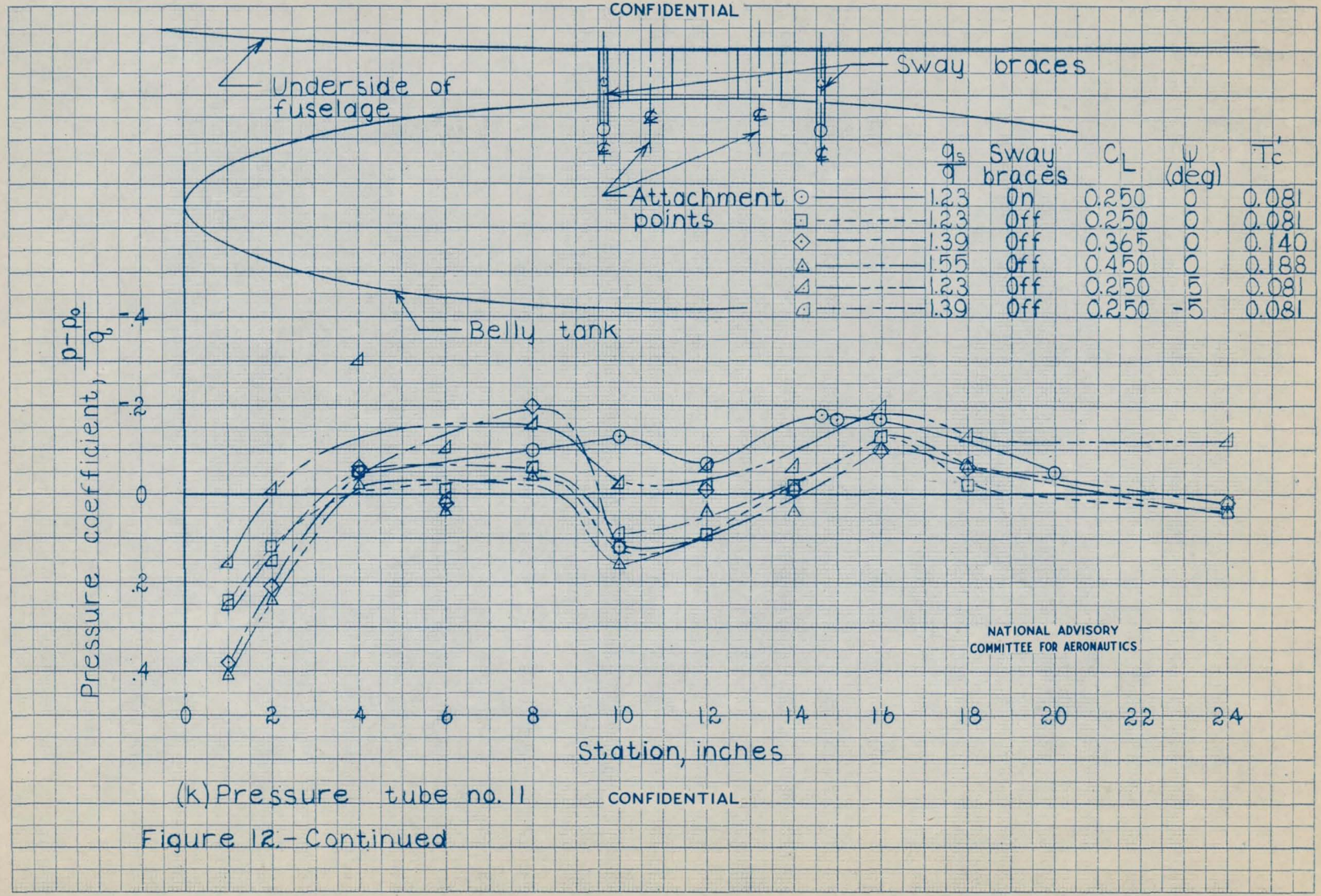

(k) Pressure tube no. 11

CONFIDENTIAL

Figure 12.- Continued

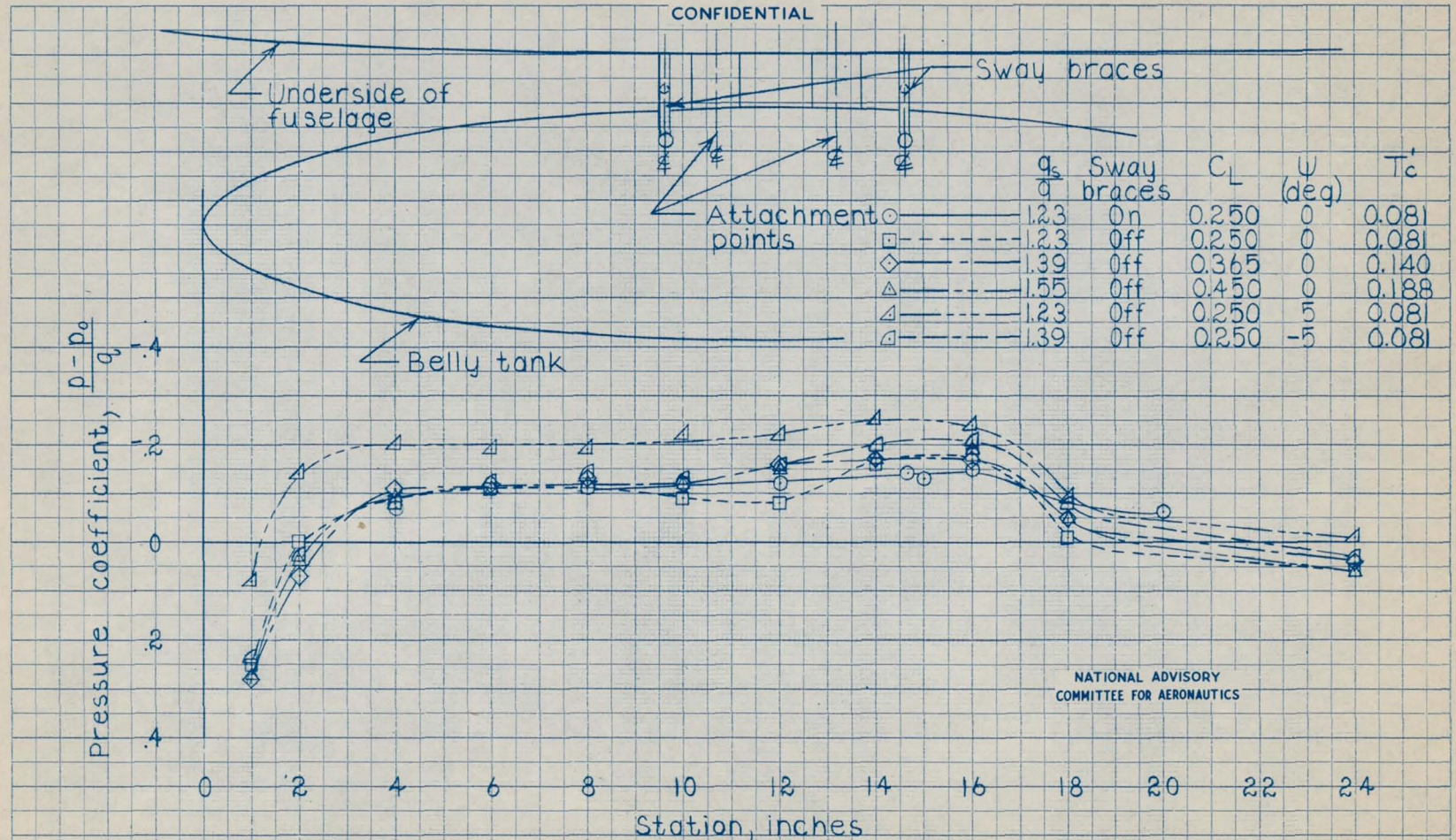

(l) Pressure tube no. 12

CONFIDENTIAL

Figure 12.- Continued

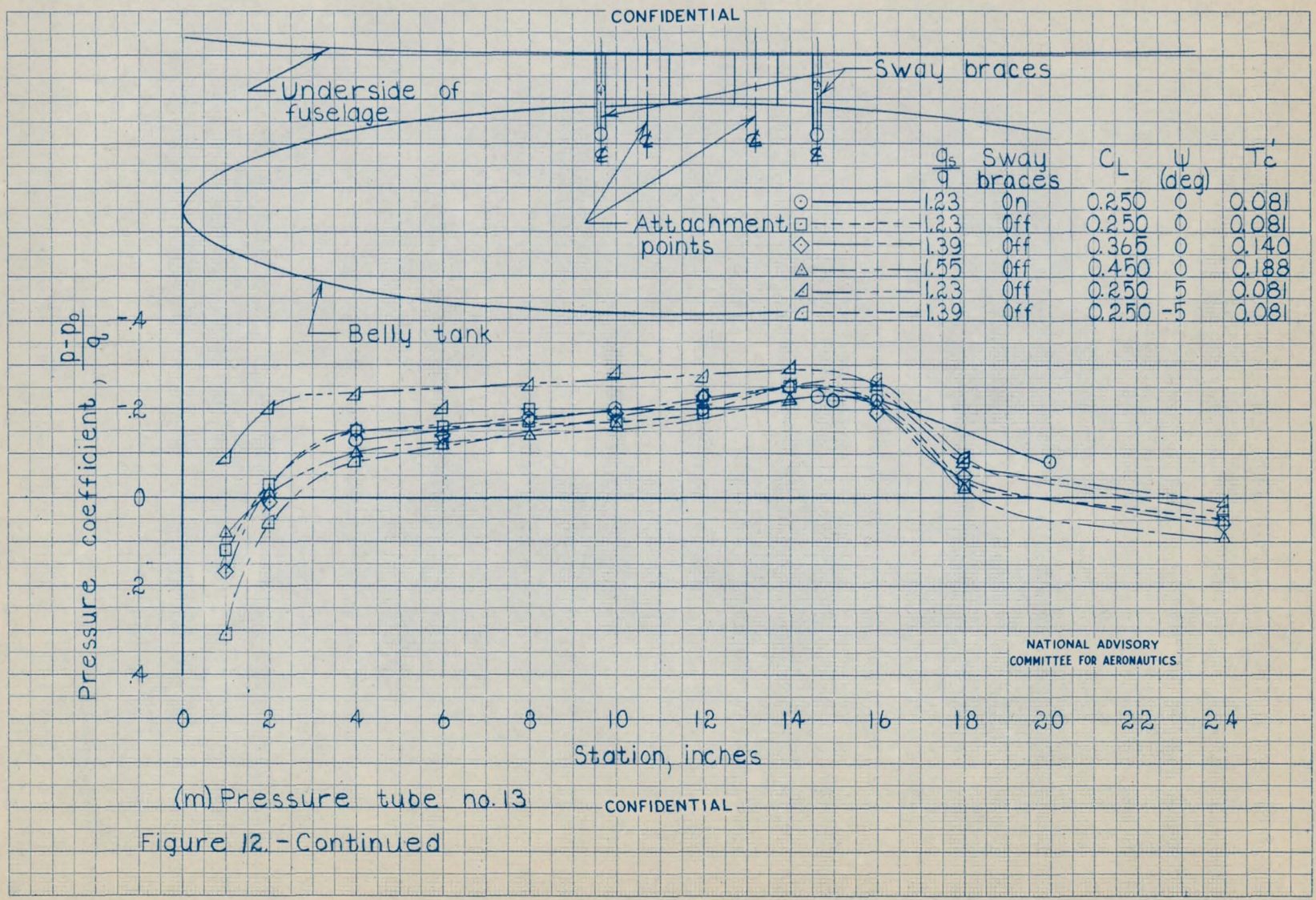

(m) Pressure tube no. 13

CONFIDENTIAL

Figure 12. - Continued

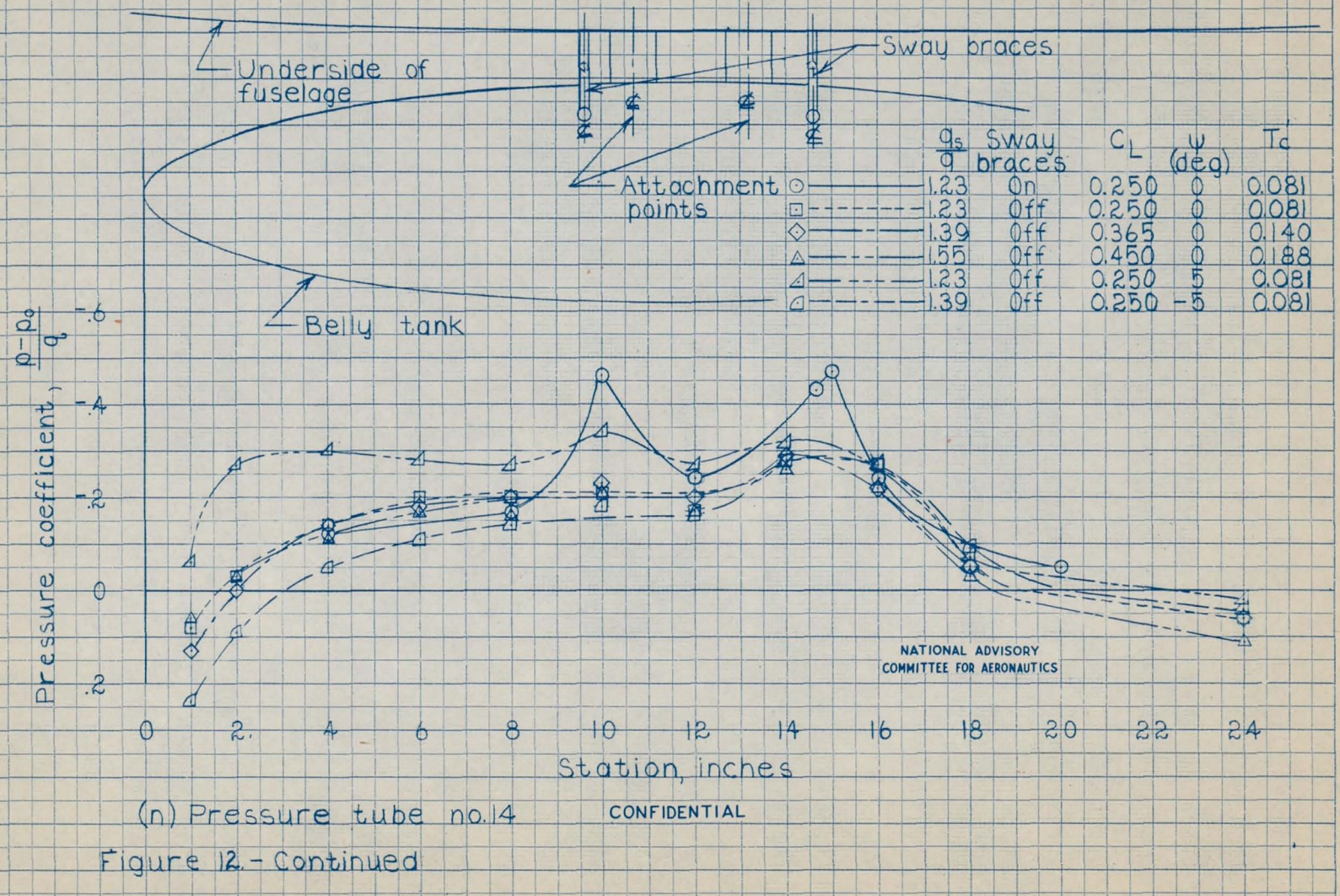

(n) Pressure tube no. 14

CONFIDENTIAL

Figure 12.- Continued

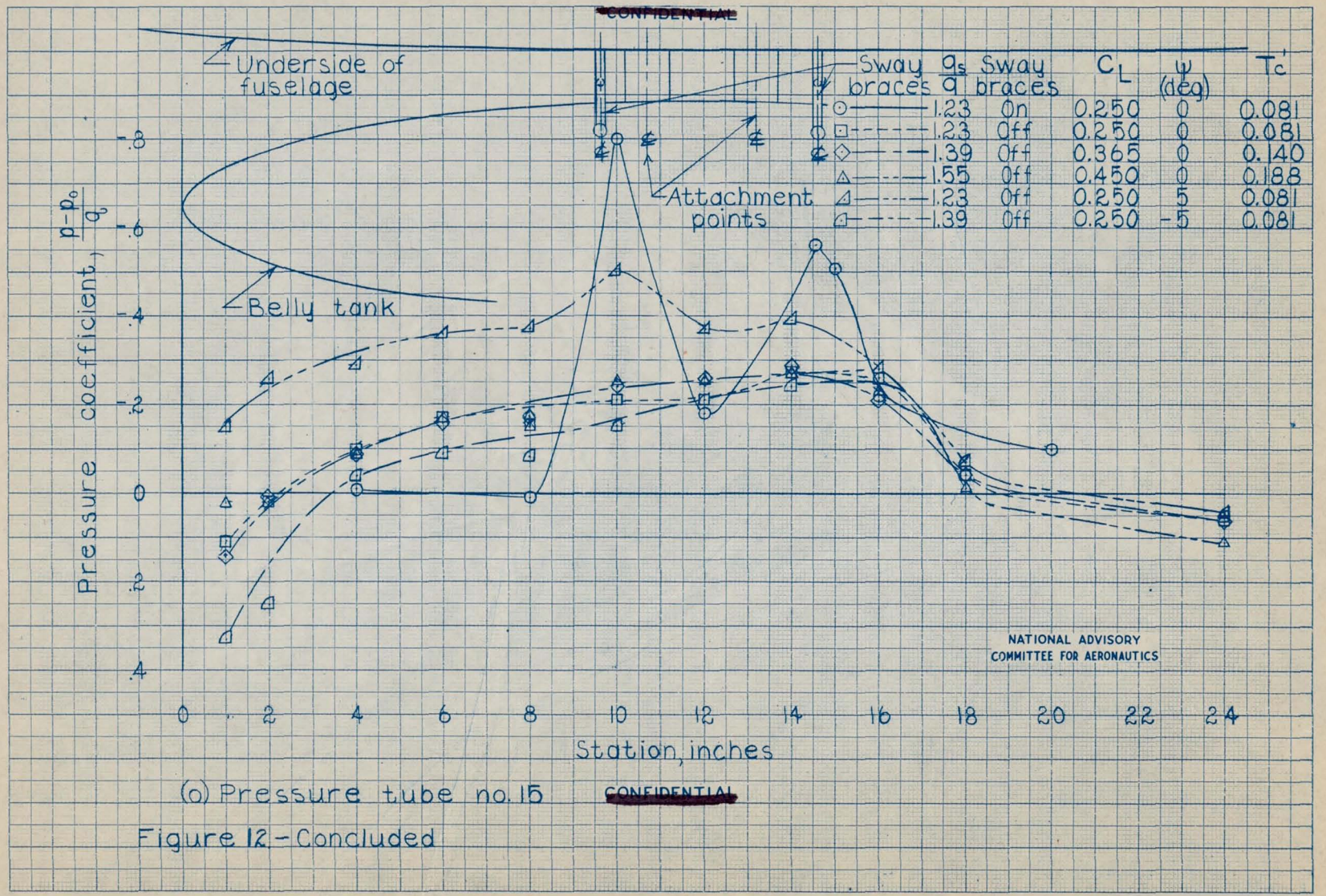

(c) Pressure tube no. 15 CONFIDENTIAL

Figure 12.- Concluded